NETWORKS AND HETEROGENEOUS MEDIA
©American Institute of Mathematical Sciences
Volume **12**, Number **3**, September **2017**
doi:10.3934/nhm.2017021
pp. **489–523**

OPINION DYNAMICS ON A GENERAL COMPACT RIEMANNIAN MANIFOLD

Aylin Aydoğdu, Sean T. McQuade and Nastassia Pouradier Duteil

Center for Computational and Integrative Biology
Rutgers University - Camden
303 Cooper Street, Camden, NJ 08102, USA

Abstract. This work formulates the problem of defining a model for opinion dynamics on a general compact Riemannian manifold. Two approaches to modeling opinions on a manifold are explored. The first defines the distance between two points using the projection in the ambient Euclidean space. The second approach defines the distance as the length of the geodesic between two agents. Our analysis focuses on features such as equilibria, the long term behavior, and the energy of the system, as well as the interactions between agents that lead to these features. Simulations for specific manifolds, $\mathbb{S}^1, \mathbb{S}^2$, and $\mathbb{T}^2$, accompany the analysis. Trajectories given by opinion dynamics may resemble $n-$body Choreography and are called "social choreography". Conditions leading to various types of social choreography are investigated in $\mathbb{R}^2$.

1. **Introduction.** The emergence of a group's global behavior from local interactions among individual agents is a fascinating feature of opinion dynamics. When local rules imply global patterns in a population, we are observing a phenomenon called *self-organization*. Traditionally, interest focuses on understanding the complex rules of interacting opinions which lead to certain global configurations, such as classic *consensus*, *alignment*, *clustering*, or the less studied *dancing equilibrium* [3]. For instance, in bounded-confidence models such as the one proposed by Hegselmann and Krause, the radius of interaction determines the clustering of the system [11]. Motsch and Tadmor studied the influence of the shape of the interaction potential on the convergence to consensus of the Hegselmann-Krause system [15]. Ha, Ha and Kim looked at the Cucker-Smale second-order alignment model and provided a condition on the interaction potential ensuring convergence of the system to alignment [9]. Cristiani, Frasca and Piccoli studied the effect of anisotropic interactions on the behavior of the group [6].

The dynamics of an opinion formation system depend on the state-space [1] and interaction network [11]. Models on the Euclidean space in one dimension (for opinion dynamics) or in two or three dimensions (with applications to groups of animals or robots) have been extensively studied and are well understood. However, such models are locally linear, which may be a limitation when one strives to capture more complex phenomena and better represent reality [21]. In this line of thought, the Kuramoto model on the sphere $\mathbb{S}^1$ addresses the problem of synchronizing a large number of oscillators [12, 22]. There exist numerous applications to this model

2010 *Mathematics Subject Classification.* Primary: 34C40; Secondary: 37N40, 91B14.
Key words and phrases. Opinion formation, consensus, multiagent systems, social choreography.

[7, 18, 19, 20]. Similarly, applications to satellite or ground vehicle coordination have motivated the development of models on special orthogonal groups [16, 17]: satellites evolve on $SO(3)$ while ground vehicles evolve on $SE(2)$ or $SE(3)$. A nonlinear model of opinion formation on the sphere was also developed in [3]. A discussion of the so called "flocking realizability problem" for a sphere is given in [5], which focuses on the particular equilibrium that we refer to as consensus for a holonomic dynamical system on a sphere.

The present work defines a general model of opinion dynamics on a Riemannian manifold. We investigate how the manifold on which the model is defined affects the global configurations resulting from opinion dynamics. These are the first steps to build a robust theory of opinion dynamics on general Riemannian manifolds.

There is an inherent difficulty in defining opinion dynamics on a general Riemannian manifold. Using the Riemannian distance, an agent will move towards a point by following the manifold's geodesics, which are well defined only locally. On a larger scale, there might not exist a unique geodesic. Another challenge is the extreme complexity of computing geodesics, even on a relatively simple manifold such as the torus [8]. One way around this issue is to consider the embedding of the manifold into a Euclidean space. Each agent's velocity is defined by projection of the other agents' influence onto the tangent space at that point. This is the choice made in [3].

Other than the mentioned practical aspect, there is an intrinsic rationale for choosing one approach over the other. When evolving along the geodesics of the manifold, one assumes that each agent has a global understanding of the manifold's geometry and is able to choose the shortest path among all possible ones. On the other hand, the approach based on the projection of the desired destination onto the tangent space implies that each agent only holds local information about the space in which it evolves. It chooses to move in the direction which locally seems to bring it closer to the target.

We explore these two specific approaches for our generalized model. The first method, Approach A, uses projections in the Euclidean space in which the manifold is embedded. The second method, Approach B, uses only geodesics defined on the manifold to define strength and direction of interaction. We exhibit properties of the interaction matrix that lead to specific kinds of equilibria. Simulations and examples compare the two methods. Dancing equilibria for Approach B are shown (dancing equilibria were studied for Approach A in [3]).

We use the sphere and torus as sample manifolds to evaluate these approaches. Specifically, we simulate dynamics on the following manifolds: $\mathbb{S}^1, \mathbb{S}^2$ and $\mathbb{T}^2$. These examples allow us to directly compare the two approaches, and see if one is more appropriate for a given manifold. We show the influence of the manifold's geometry on the dynamics by examining the dynamics resulting from the same interaction matrix in $\mathbb{S}^2$, $\mathbb{T}^2$ and $\mathbb{R}^2$.

Opinion dynamics trajectories can resemble $n-$body choreography, that is, solutions to the well known $n-$body problem. These dynamics drive agents along orbits which either are periodic, or have a periodic feature, and that may be shared by multiple agents. We refer to opinion dynamics trajectories along such orbits as "Social Choreography". We show that a simple example of Social Choreography in $\mathbb{R}^2$ does not hold on $\mathbb{S}^2$ or $\mathbb{T}^2$, see Figures 10 and 11. We then focus on the case of $\mathbb{R}^2$ and investigate initial conditions and properties of the interaction matrix which

give rise to Social Choreography. Future investigations can consist of exploring similar properties of trajectories on general manifolds.

2. **Choice of the model.** This work will primarily discuss two approaches to define opinion dynamics on a Riemannian manifold. Let M be a Riemannian manifold. Let $N \in \mathbb{N}$ represent the number of agents with opinions evolving on M. We denote by $x := (x_i)_{i\in\{1,\dots,N\}} \in M^N$ the set of opinions. For each $i \in \{1, ..., N\}$, $\dot{x}_i \in T_{x_i}M$. The opinions x_i evolve according to the following general dynamics:

$$\dot{x}_i = \sum_{j=1}^{N} a_{ij}\Psi(d(x_i, x_j))\nu_{ij} \tag{1}$$

where

- $a_{ij} \in \mathbb{R}$ is the interaction coefficient of the pair of agents i and j,
- $\Psi : \mathbb{R} \to \mathbb{R}$ is the interaction potential,
- $d(\cdot, \cdot) : M \times M \to \mathbb{R}^+$ represents the distance between opinions,
- $\nu_{ij} \in T_{x_i}M$ is a unit vector giving the direction of the influence of j over i.

Each of these terms is further specified in the following.

2.1. **Approaches.** The evolution of each agent's opinion depends on the opinions of all other agents, with influences weighted by the interaction coefficients a_{ij}. More specifically, an agent x_j's influence on x_i is determined by two elements: the direction of influence $\nu_{ij} \in T_{x_i}M$ and the magnitude of influence $\Psi(d(x_i, x_j)) \in \mathbb{R}^+$. We propose and study two different approaches for the choices of d and ν_{ij}. Approach A uses the embedding of M in $\mathbb{R}^n$ to define $d(x_i, x_j)$, whereas Approach B is intrinsic to M, with distance and direction of influence based on geodesics.

Approach A. Assume that M of dimension m is embedded in a Euclidean space $\mathbb{R}^n$, with $n \geq m$. Agent x_j acts on agent x_i via a projection onto $T_{x_i}M \subset \mathbb{R}^m$. Now considering points $(x_i, x_j) \in M^2$ as points of $\mathbb{R}^n$, the difference $x_j - x_i$ is a vector of $\mathbb{R}^n$. Given a vector subspace Y of $\mathbb{R}^n$, we denote by $\Pi_Y y$ the projection of $y \in \mathbb{R}^n$ onto $Y \subset \mathbb{R}^n$ and define $d_P(\cdot, \cdot)$ as follows:

$$d_P(x_i, x_j) = \|\Pi_{T_{x_i}M}(x_j - x_i)\| \tag{2}$$

where $\|\cdot\|$ denotes the Euclidean norm on $\mathbb{R}^n$. The same projection also defines the direction of influence of x_j on x_i:

$$\nu_{ij} = \begin{cases} \frac{\Pi_{T_{x_i}M}(x_j - x_i)}{\|\Pi_{T_{x_i}M}(x_j - x_i)\|} & \text{if } \Pi_{T_{x_i}M}(x_j - x_i) \neq 0 \\ 0 \quad \text{otherwise.} \end{cases} \tag{3}$$

With the specific choice $\Psi \equiv \mathrm{Id}$, system (1)-(2)-(3) becomes:

$$\dot{x}_i = \sum_{j=1}^{N} a_{ij}\Pi_{T_{x_i}M}(x_j - x_i). \tag{4}$$

This is the approach used in [3], applied to the sphere $\mathbb{S}^2$.

Notice that the magnitude of influence, $d_P(x_i, x_j)$, is symmetric for the sphere in the sense that $d_P(x_i, x_j) = d_P(x_j, x_i)$, but not symmetric for a general Riemannian manifold (see Figure 1). However, it is a continuous function defined for all pairs of points $(x_i, x_j) \in M^2$. The originality of this approach is that the influence of x_j on x_i is not related to a notion of distance between the points. The use of the projection of $x_j - x_i$ onto $T_{x_i}M$ reflects the concept of "local visibility." For the situation of

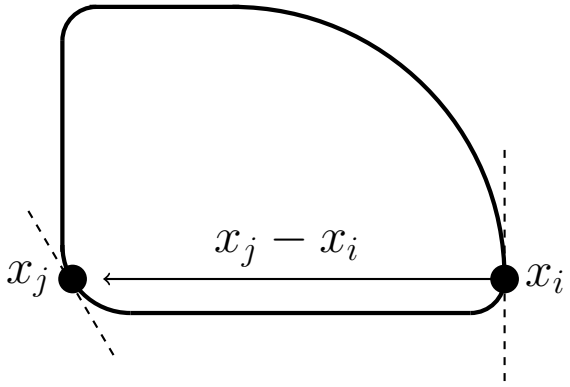

FIGURE 1. An example of a manifold M such that $d_p(x_i, x_j) \neq d_p(x_j, x_i)$, Using system (4), an agent is subject to "local visibility", and movement of x_i along $T_{x_i}M$ (dashed line through x_i) will not bring x_i closer to x_j in this local sense.

two agents evolving on a one dimensional manifold, if $x_j - x_i \perp T_{x_i}M$, then a local displacement of x_i does not affect the distance between the points $\|x_i - x_j\|$. Indeed, a first order Taylor expansion gives: $x_i(\varepsilon) = x_i(0) + \varepsilon \dot{x}_i(0) + o(\varepsilon)$.

Supposing that x_j is fixed, we have:

$$\begin{aligned} \|x_i(\varepsilon) - x_j\|^2 &= \langle x_i(\varepsilon) - x_j, x_i(\varepsilon) - x_j \rangle \\ &= \langle x_i(0) - x_j, x_i(0) - x_j \rangle + 2\varepsilon \langle \dot{x}_i(0), x_i(0) - x_j \rangle + o(\varepsilon) \end{aligned} \tag{5}$$

so if $x_j - x_i(0) \perp T_{x_i(0)}M$, then $\|x_i(\varepsilon) - x_j\|^2 = \|x_i(0) - x_j\|^2 + o(\varepsilon)$. Hence if x_i only has local visibility, all directions of displacement seem equivalent (at first order), which justifies the influence of x_j over x_i to be zero if their difference is orthogonal to the tangent space of M at x_i. This is illustrated in Figure 1.

Approach B. This second approach defines d and ν_{ij} using the manifold M itself, and does not require any reference to the space in which M is immersed. This would make Approach B a natural way to define system dynamics, however the complete knowledge of the geodesics between any two points on the manifold may be unrealistic. Furthermore, the geometry of the manifold may introduce difficulties to the uniqueness of ν_{ij}, particularly at the cut-locus of a point.

Definition 2.1. The **cut locus** of a point $q \in M$ is the set of points $\mathcal{CL}(q) \subset M$ for which there are multiple geodesics between q and $p \in \mathcal{CL}(q)$ (see also [4]).

Let $\gamma_{ij} : [0,1] \to M$ denote a geodesic connecting x_i to $x_j, \gamma_{ij}(0) = x_i$ and $\gamma_{ij}(1) = x_j$. We then define the distance between x_j and x_i as the length of a geodesic, i.e. denoting by $g_y : T_yM \times T_yM \to \mathbb{R}^+$ the Riemannian metric at point $y \in M$,

$$d_G(x_i, x_j) = \int_0^1 \sqrt{g_{\gamma_{ij}(s)}(\dot{\gamma}_{ij}(s), \dot{\gamma}_{ij}(s))} ds. \tag{6}$$

The direction of influence is determined by the same geodesic:

$$\nu_{ij} = \begin{cases} 0 & \text{if } x_j = x_i \text{ or if } x_j \in \mathcal{CL}(x_i) \\ \frac{\dot{\gamma}_{ij}(0)}{\sqrt{g_{x_i}(\dot{\gamma}_{ij}(0), \dot{\gamma}_{ij}(0))}} & \text{otherwise.} \end{cases} \tag{7}$$

Unlike in Approach A, the magnitude of influence is a symmetric function: $d_G(x_i, x_j) = d_G(x_j, x_i)$. Furthermore, this approach ensures that the magnitude of influence of one agent on another is a function of the exact Riemannian distance between the agents.

Interaction networks. In finite-dimensional systems such as system (1), the set of interacting agents can be described by vertices of a graph. A directed edge exists from a vertex i to a vertex j if and only if $a_{ij} \neq 0$. The system depends on the interaction network, and likewise, if the coefficients a_{ij} are chosen to be functions of the state, the interaction network may change as a result of the dynamics. Two main types of interaction networks have been proposed in the literature: metric interactions and topological interactions. If interactions between agents occur only locally, only the neighbors of agent i influence agent i. Metric interactions define the set of neighbors of agent i, given a radius $r > 0$, as

$$\mathcal{S}_i^r(x) = \{j \in \{1, \ldots, N\}, d(x_i, x_j) \leq r\}, \tag{8}$$

where $d(\cdot, \cdot)$ can represent either the projection or the geodesic distance, as specified in each of the two approaches described above (see equations (2) and (6)). The other main type of interactions specifies that an agent is influenced by only its k closest neighbors. We call these topological interactions [1]. We define the relative separation between two agents as $\alpha_{ij} = \mathbf{card}\{k : d(x_i, x_k) \leq d(x_i, x_j)\}$, The set of neighbors of agent i is then defined as the set of its k closest neighbors, i.e. for a given $k \in \mathbb{N}$,

$$\mathcal{S}_i^k(x) = \{j \in \{1, \ldots, N\}, \alpha_{ij} \leq k\}. \tag{9}$$

Figures 2 and 3 illustrate differences between the metric and topological networks for the specific example of $\mathbb{S}^1$, with each of the approaches A and B.

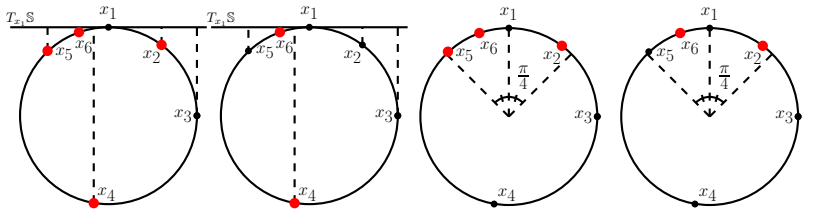

(A) Approach A metric, $r = \frac{\pi}{4}$

(B) Approach A topological, $k = 2$

(C) Approach B metric, $r = \frac{\pi}{4}$

(D) Approach B topological, $k = 2$

FIGURE 2. The set of agents that influence x_1 depends on how the interaction network is defined. In (a) and (b) the dashed lines show the projection of agents onto the tangent space of x_i, $(T_{x_i}\mathbb{S}^1)$. The agents depicted in red with larger dots influence x_1. With the same configuration on $\mathbb{S}^1$, four combinations are possible (approach {A,B} type {Metric, Topological}). Each combination implies x_1 interacts with a different set of agents.

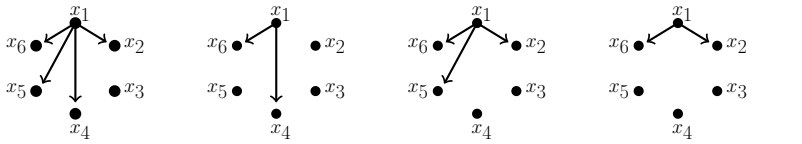

(A) Approach A metric, $r = \frac{\pi}{4}$ (B) Approach A topological, $k = 2$ (C) Approach B metric, $r = \frac{\pi}{4}$ (D) Approach B topological, $k = 2$

FIGURE 3. The agent x_1 is influenced by different agents depending on how the interaction network is defined. These networks may change as the dynamics move the agents on $\mathbb{S}^1$. Each agent $x_j, j \in \{1, \dots, 6\}$ will have a network describing which other agents influence x_j. The interaction networks corresponding to systems from Figure 2.

Resolution of discontinuities. The definitions of ν_{ij} for approaches A and B (given by equations (3) and (7)) allow discontinuities of ν_{ij} at certain points. Thus, one must impose conditions on the interaction potential $\Psi \in \mathcal{C}^0(\mathbb{R}^+, \mathbb{R}^+)$, in order to ensure the continuity of the right-hand side of the system (1), and hence the existence and uniqueness of a solution. Table 1 lists the discontinuities of ν_{ij} and gives necessary conditions on Ψ to ensure the continuity of $\Psi(d(x_i, x_j))\nu_{ij}$.

Firstly, notice that in both approaches, ν_{ij} is discontinuous at the point $x_i = x_j$. Indeed, if $x_i = x_j$, $\nu_{ij} = 0$, whereas almost everywhere else, $\|\nu_{ij}\| = 1$. To ensure the continuity of $\Psi(d(x_i, x_j))\nu_{ij}$ at this point, we impose the following condition:

$$\Psi(0) = 0. \tag{10}$$

In Approach A, we created a discontinuity of ν_{ij} at the points $x_j \in \mathcal{N}(x_i)$, where we denote by $\mathcal{N}(q)$ the set $\mathcal{N}(q) := \{q \in M \mid \Pi_{T_pM}(q - p) = 0\}$. For convenience of notation, we will use interchangeably the notations $\mathcal{N}(x_i)$ and $\mathcal{N}_i$. More specifically, we have $\lim_{x_j \to \mathcal{N}_i} \|\nu_{ij}\| = 1$ but $\|\nu_{ij}\| = 0$ if $x_j \in \mathcal{N}_i$ (see also Table 1). However, from the definition of d_P (see equation (2)), we have $\lim_{x_j \to \mathcal{N}_i} d_P(x_i, x_j) = 0$ and $d(x_i, x_j) = 0$ for $x_j \in \mathcal{N}_i$. Hence a sufficient condition for $\Psi(d(x_i, x_j))\nu_{ij}$ to be continuous is again:

$$\Psi(0) = 0. \tag{11}$$

In Approach B, there is a discontinuity for $x_j \in \mathcal{CL}(x_i)$. Denoting by $B^{\text{geo}}(p, \rho)$ the geodesic ball of center p and radius ρ, we require the following condition on the influence function Ψ:

$$\Psi(d) = 0 \text{ for all } d \geq \epsilon \tag{12}$$

where $\epsilon := \inf\{\rho > 0 \mid \forall p \in M, B^{\text{geo}}(p, \rho) \cap \mathcal{CL}(p) = \emptyset\}$. This distance ϵ, also known as injectivity radius, is known to exist and be greater than 0 for any compact Riemannian manifold (see [4]).

Approach	A	B	A and B
Critical points	$x_j \in \mathcal{N}_i$	$x_j \in \mathcal{CL}(x_i)$	$x_j = x_i$
Discontinuities	$\lim_{x_j \to \mathcal{N}_i} \|\nu_{ij}\| = 1$ $\|\nu_{ij}\| = 0$ for $x_j \in \mathcal{N}_i$	$\lim_{x_j \to \mathcal{CL}(x_i)} \|\nu_{ij}\| = 1$ $\|\nu_{ij}\| = 0$ for $x_j \in \mathcal{CL}(x_i)$	$\lim_{x_j \to x_i} \|\nu_{ij}\| = 1$ $\|\nu_{ii}\| = 0$
Condition on Ψ	$\Psi(0) = 0$	$\Psi(d) = 0$ for all $d \geq \epsilon$	$\Psi(0) = 0$

TABLE 1. Possible discontinuities of the right-hand side of (1). The bottom row of the table show conditions for Ψ so that the system is continuous.

Notice that in the case of the geodesics approach (Approach B), the condition $\Psi(d) = 0$ for all $d \geq \epsilon$ is incompatible with the use of the topological network (9). Indeed, if agent j is among the k closest neighbors of agent i, the topological network would require: $a_{ij} \neq 0$. However, the interaction between i and j would be canceled if $d_G(x_i, x_j) > \epsilon$. On the other hand, the metric interaction network as defined by (8) is compatible with Approach A, and with Approach B if the interaction radius is smaller than the injectivity radius: $r \leq \epsilon$. For simplicity purposes, in the rest of this paper, we will consider that the interaction coefficients a_{ij} are constant, thus not requiring the need to differentiate between metric and topological networks. While models with constant interaction coefficients are our focus here, these models are quite restrictive, and exclude all models with dynamic interactions.

2.2. **Definitions and general results.**

Definition 2.2. The configuration $x_1 = ... = x_N$ is called **consensus**. On the sphere, $\mathbb{S}^n$, A configuration such that, for every $j \in \{2, \dots, N\}$, *either* $x_j = x_1$ *or* $x_j = -x_1$, which is not a concensus is called **antipodal equilibrium**.

Proposition 1. *The consensus configuration is an equilibrium for system* (1).

Proof. In both approaches A and B, if $x_i = x_j$, then $\nu_{ij} = 0$. Hence if $x_1 = ... = x_N$, then for all $i \in \{1, \dots, N\}$, $\dot{x}_i = 0$. □

Proposition 2. *Let* $N > d + 1$. *Then for every* $\bar{x} = (\bar{x}_1, \dots, \bar{x}_N) \in M^N$, *there exists a square matrix* $A = (a_{ij})_{i,j \in \{1,\dots,N\}}$ *such that* $\bar{x}$ *is an equilibrium for system* (1).

Proof. The configuration $\bar{x} = (\bar{x}_1, \dots, \bar{x}_N)$ is an equilibrium if and only if

$$\frac{d}{dt}\bar{x}_i = \sum_{j=1}^{N} a_{ij}\Psi(d(\bar{x}_i, \bar{x}_j))\nu_{ij} = 0.$$

This is a system of at most Nd equations in the $N^2 - N$ unknowns a_{ij}, $i \neq j$, notice that $\Psi(d(x_i, x_i)\nu_{ii} = 0$, and diagonal values of A do not change the system. So if $N > d + 1$ there exists a nontrivial choice of the interaction coefficients for which $\bar{x}$ is an equilibrium. □

Definition 2.3. The kinetic energy of System (1)-(2)-(3) is the quantity

$$E_P(t) := \frac{1}{2}\sum_{i=1}^{N} \|\dot{x}_i(t)\|^2. \tag{13}$$

The kinetic energy of System (1)-(6)-(7) is the quantity

$$E_G(t) := \frac{1}{2}\sum_{i=1}^{N} g_{x_i}(\dot{x}_i(t), \dot{x}_i(t)). \tag{14}$$

Proposition 3. *Let M be a general Riemannian compact manifold. Consider the dynamics given by projection onto the tangent space (Approach A) given by (4). If the interaction matrix $A = (a_{ij})_{i,j\in\{1,\dots,N\}^2}$ is symmetric, then*

$$\lim_{t\to\infty} E_P(t) = 0. \tag{15}$$

Proof. Let $F(t) = \frac{1}{2}\sum_{i=1}^{N}\sum_{j=1}^{N} a_{ij}\|x_i - x_j\|^2$. Using the symmetry of A, we prove that

$$\frac{d}{dt}F(t) = 4E_P(t). \tag{16}$$

Indeed, notice that

$$\nabla_{x_i}\Big(\sum_{j=1}^{N} a_{ij}\|x_i - x_j\|^2\Big) = 2\Pi_{T_{x_i}M}\sum_{j=1}^{N} a_{ij}(x_j - x_i) = 2\dot{x}_i.$$

Then we compute

$$\begin{aligned}
\frac{d}{dt}F(t) &= \sum_{k=1}^{N}\langle \nabla_{x_k}\frac{1}{2}\sum_{i,j=1}^{N} a_{ij}(\|x_i - x_j\|^2), \dot{x}_k\rangle \\
&= \sum_{k=1}^{N}\langle \nabla_{x_k}\left[\frac{1}{2}\sum_{i=1}^{N} a_{ik}(\|x_i - x_k\|^2) + \frac{1}{2}\sum_{j=1}^{N} a_{kj}(\|x_k - x_j\|^2)\right], \dot{x}_k\rangle \\
&= \sum_{k=1}^{N}\langle 2\nabla_{x_k}\frac{1}{2}\sum_{i=1}^{N} a_{ik}(\|x_i - x_k\|^2), \dot{x}_k\rangle = \sum_{k=1}^{N}\langle 2\Pi_{T_{x_k}M}\sum_{j=1}^{N} a_{kj}(x_j - x_k), \dot{x}_k\rangle \\
&= 2\sum_{k=1}^{N}\|\dot{x}_k\|^2 = 4E_P(t).
\end{aligned} \tag{17}$$

where the third equality uses the property: $a_{ij} = a_{ji}$ for all i, j.

Since $E_P(t) \geq 0$, $F(t)$ is a non-decreasing function. Moreover $F(t)$ and $\frac{d^2}{dt^2}F(t)$ are bounded, since M is a compact manifold. Hence $F(t)$ converges as $t \to \infty$.

Now, $\int_0^{+\infty} E_P < \infty$ and there exists $c > 0$ such that $\sup_t \frac{d}{dt}E_P(t) < c$. By contradiction, assume $\limsup E_P = \alpha > 0$, then there exists a sequence (t_n) such that $t_{n+1} > t_n + \frac{\alpha}{2c}$ and $E_P(t_n) \geq \frac{\alpha}{2}$. Then $\int_0^{\infty} E_P > \sum_n \frac{\alpha}{c}\cdot\frac{\alpha}{2}\cdot\frac{1}{2} = +\infty$. Hence $\limsup_t E_P(t) = 0$.

This shows that $\frac{d}{dt}F(t) \to 0$ when $t \to \infty$, which implies that $\lim_{t\to\infty} E_P(t) = 0$. □

Remark 1. Propositions 2 and 3 are generalizations of results proven for the case $M = \mathbb{S}^2$ in [3].

Remark 2. Proposition 3 assumes that $\Psi \equiv \mathrm{Id}$ which creates a discontinuity for Approach B (see Table 1). A result is shown for the more restricted case of $M = \mathbb{S}^2$ and $\Psi(\cdot) \equiv \sin(\cdot)$, (Corollary 1).

Definition 2.4. Let x solve the differential equation (1). A *dancing equilibrium* is a configuration in which for all pairs of agents (i,j), the distance $d_P(x_i,x_j)$ (in Approach A) or $d_G(x_i,x_j)$ (in Approach B) is constant. In the context of a system of oscillators, this equilibrium is also known as a phase-locked state or entrainment state [10].

Remark 3. This definition is a generalization of the concept of *dancing equilibrium* described in [3].

Remark 4. It follows immediately from definition 2.4 that the kinetic energy of a system in dancing equilibrium is constant.

3. Analysis and simulations on $\mathbb{S}^1$.

3.1. **Models.** We study both approaches A and B in the case $M=\mathbb{S}^1$, i.e. for the one-dimensional sphere embedded in $\mathbb{R}^2$. Let $(\theta_i)_{i\in\{1,\dots,N\}}\in[0,2\pi]^N$ such that for all $i\in\{1,...,N\}$, $x_i=(\cos\theta_i,\sin\theta_i)^T$.
Approach A. The projection onto an agent's tangent space can be rewritten as:

$$\begin{aligned}\Pi_{T_{x_i}}\sum_{j=1}^N a_{ij}(x_j-x_i) &= \sum_{j=1}^N a_{ij}\langle\begin{pmatrix}\cos\theta_j\\ \sin\theta_j\end{pmatrix}-\begin{pmatrix}\cos\theta_i\\ \sin\theta_i\end{pmatrix},\begin{pmatrix}-\sin\theta_i\\ \cos\theta_i\end{pmatrix}\rangle\begin{pmatrix}-\sin\theta_i\\ \cos\theta_i\end{pmatrix}\\ &=\sum_{j=1}^N a_{ij}(-\sin\theta_i\cos\theta_j+\sin\theta_j\cos\theta_i)\begin{pmatrix}-\sin\theta_i\\ \cos\theta_i\end{pmatrix}\\ &=\sum_{j=1}^N a_{ij}\sin(\theta_j-\theta_i)\begin{pmatrix}-\sin\theta_i\\ \cos\theta_i\end{pmatrix}.\end{aligned}\tag{18}$$

So System (1)-(2)-(3) becomes:

for all$i\in\{1,\dots,N\}$,

$$\dot\theta_i\begin{pmatrix}-\sin\theta_i\\ \cos\theta_i\end{pmatrix}=\sum_{j=1}^N a_{ij}\Psi(|\sin(\theta_j-\theta_i)|)\operatorname{sgn}(\sin(\theta_j-\theta_i))\begin{pmatrix}-\sin\theta_i\\ \cos\theta_i\end{pmatrix}\tag{19}$$

where $\operatorname{sgn}(\cdot)$ is the sign function defined by:

$$\text{for all } x\in\mathbb{R},\quad \operatorname{sgn}(x)=\begin{cases}1 & \text{if } x>0\\ -1 & \text{if } x<0\\ 0 & \text{if } x=0.\end{cases}\tag{20}$$

We can then specify:

$$\text{for all } (i,j)\in\{1,\dots,N\}^2,\quad d_P(x_i,x_j)=|\sin(\theta_j-\theta_i)|,\quad \nu_{ij}^P=\operatorname{sgn}(\sin(\theta_j-\theta_i)).\tag{21}$$

This gives the system of scalar equations:

$$\text{for all } i\in\{1,\dots,N\},\quad \dot\theta_i=\sum_{j=1}^N a_{ij}\Psi(|\sin(\theta_j-\theta_i)|)\operatorname{sgn}(\sin(\theta_j-\theta_i)).\tag{22}$$

In particular, in the case $\Psi\equiv\mathrm{Id}$, the system becomes the Kuramoto model [12].

$$\text{for all } i\in\{1,\dots,N\},\quad \dot\theta_i=\sum_{j=1}^N a_{ij}\sin(\theta_j-\theta_i).\tag{23}$$

Approach B. For $M = \mathbb{S}^1$, the geodesics distance d_G and the vector ν_{ij}^G are given by:

$$d_G(x_i, x_j) = \arccos(\cos(\theta_j - \theta_i)) \quad , \quad \nu_{ij}^G = \operatorname{sgn}(\sin(\theta_j - \theta_i)). \tag{24}$$

System (1)-(6)-(7) is written:

$$\text{for all } i \in \{1, \dots, N\}, \quad \dot{\theta}_i = \sum_{j=1}^{N} a_{ij} \Psi(\arccos(\cos(\theta_j - \theta_i))) \operatorname{sgn}(\sin(\theta_j - \theta_i)). \tag{25}$$

In order for the system to be well defined, the interaction function Ψ must satisfy the conditions given in Table 1. Notice that the injectivity radius is constant over $\mathbb{S}^1$, with $\epsilon = \pi$. Possible choices involve choosing Ψ from a family of function defined as follows:

$$\Psi^a(d) = \begin{cases} \frac{1}{a} d & \text{for } d \leq a \\ \frac{d-\pi}{a-\pi} & \text{for } d > a \end{cases} \tag{26}$$

where $a \in (0, \pi)$ (see Figure 8).

Another possible choice is: $\Psi : x \mapsto \sin(x)$. Notice that for the specific choices $\Psi = \mathrm{Id}$ for Approach A and $\Psi : x \mapsto \sin(x)$ for Approach B, the two approaches A and B are equivalent.

3.2. **Analysis.** We first examine the different equilibria for both approaches.

Theorem 3.1. *Consider Approach A, System (22). Let $N \in \mathbb{N}$ be even. Suppose that for all $i \in \{1, \dots, N\}$ for all $j \in \{1, \dots \frac{N}{2}\}$, $a_{ij} = a_{i(j+\frac{N}{2})}$. Then any configuration that is centrally symmetric, i.e.*

$$\text{for all } j \in \{1, \dots, \frac{N}{2}\}, \ \theta_{j+\frac{N}{2}} = \theta_j + \pi$$

is an equilibrium.

Proof. Using the hypotheses from Theorem 3.1, we can easily compute:

$$\begin{aligned}
\dot{\theta}_i &= \sum_{j=1}^{N} a_{ij} \Psi(\|\sin(\theta_j - \theta_i)\|) \operatorname{sgn}(\sin(\theta_j - \theta_i)) \\
&= \sum_{j=1}^{N/2} [a_{ij} \Psi(\|\sin(\theta_j - \theta_i)\|) \operatorname{sgn}(\sin(\theta_j - \theta_i)) + \\
&\qquad a_{i(j+\frac{N}{2})} \Psi(\|\sin(\theta_{j+\frac{N}{2}} - \theta_i)\|) \operatorname{sgn}(\sin(\theta_{j+\frac{N}{2}} - \theta_i))] \\
&= \sum_{j=1}^{N/2} [a_{ij} \Psi(\|\sin(\theta_j - \theta_i)\|) \operatorname{sgn}(\sin(\theta_j - \theta_i)) + \\
&\qquad a_{ij} \Psi(\|\sin(\theta_j + \pi - \theta_i)\|) \operatorname{sgn}(\sin(\theta_j + \pi - \theta_i))] = 0.
\end{aligned}$$

□

Interestingly, Theorem 3.1 is not applicable to Approach B. We illustrate the different behaviors of the two systems by studying the specific example of four agents initially in a rectangular configuration. According to Theorem 3.1, this configuration is an equilibrium for Approach A, independently of the choice of interaction function Ψ. However, one can easily prove that in the geodesics-based Approach B, with $N = 4$ and the choice $\Psi := \Psi^a$ with $a = \frac{3\pi}{4}$, the only equilibrium for which all agents have pairwise distinct positions is obtained by a regular polygon,

i.e. all agents are evenly spaced out on the circle. This is illustrated by numerical simulations shown in Figure 4.

This highlights the fundamentally different behaviors of the systems (1)-(2)-(3) and (1)-(6)-(7) in the case $M = \mathbb{S}^1$.

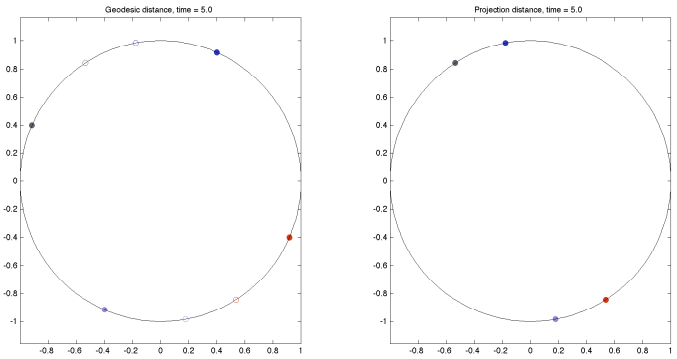

FIGURE 4. Initial (empty circles) and final positions (filled circles) of 4 agents initially on the vertices of a rectangle with Approach B (left) and Approach A (right), with $A = \mathbb{1}$, $\Psi \equiv \mathrm{Id}$ (Approach A) and $\Psi = \Psi^{3\pi/4}$(Approach B) (see equation (26)). Notice that with Approach A, initial and final positions are identical since any rectangle configuration is an equilibrium. However, with Approach B, the system reaches a square configuration, the only possible equilibrium with pairwise distinct positions.

In both approaches A and B, conditions on the interaction matrix A can be found such that the system forms a dancing equilibrium (see Definiton 2.4).

Theorem 3.2. *Consider the dynamics on* $\mathbb{S}^1$ *given by:*

$$\text{for all } i \in \{1, \dots, N\}, \quad \dot{\theta}_i = \sum_{j=1}^{N} a_{ij} \Psi(d(x_i, x_j)) \nu_{ij} \tag{27}$$

where $d(\cdot,\cdot)$ *and* ν *are given either by Approach A* (21) *or Approach B* (24)*. Let* $C \in \mathbb{R}$ *and suppose that for all* $i \in \{1, \dots, N\}$*,*

$$a_{ij} = \begin{cases} \frac{C}{\Psi(d(x_i(0), x_j(0)))} \nu_{ij} & \text{if } \Psi(d(x_i(0), x_j(0))) \neq 0 \\ 0 & \text{otherwise.} \end{cases} \tag{28}$$

Then the system is in a dancing equilibrium.

Proof. If the interaction matrix satisfies (28), then at $t = 0$,

$$\text{for all } i \in \{1, \dots, N\}, \quad \dot{\theta}_i(0) = \sum_{j=1}^{N} C = CN$$

so for all $(i, j) \in \{1, \dots, N\}^2$, $\dot{\theta}_i(0) - \dot{\theta}_j(0) = 0$. Then $d(x_i, x_j)$ does not change in time, and (28) holds for all time. □

Numerical simulations show the evolution of the system (27) with condition (28) for the projection or the geodesic distance, see Figures 5 and 6.

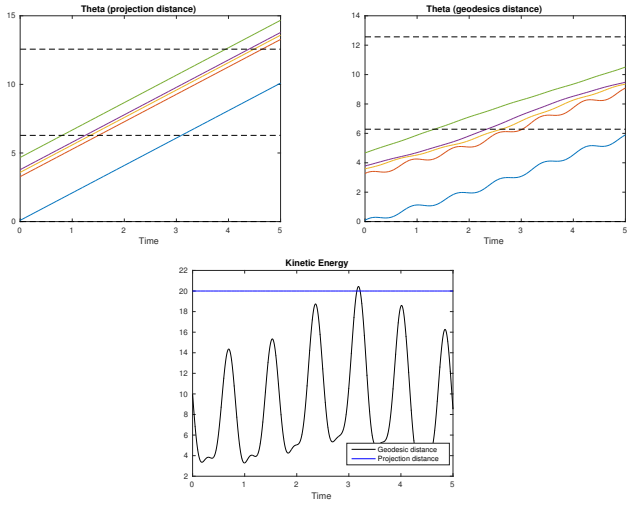

FIGURE 5. Evolution of the system (27) with Approach A (left) Approach B (center) when the interaction matrix satisfies condition (28) for the projection distance. Right: Kinetic energy.

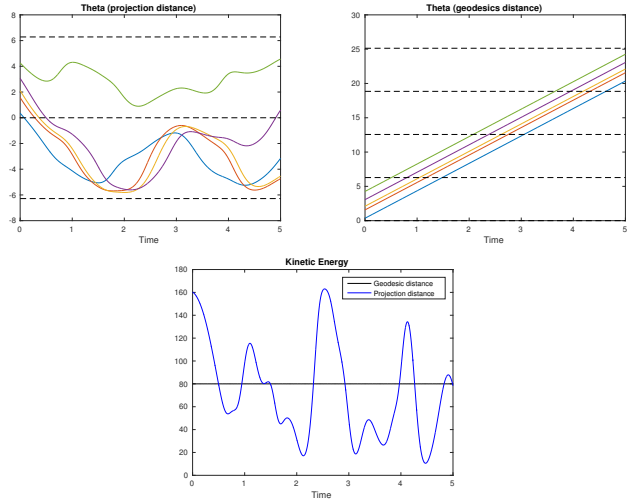

FIGURE 6. Evolution of the system (27) with Approach A (left) Approach B (center) when the interaction matrix satisfies condition (28) for the geodesic distance. Right: Kinetic energy.

4. **Analysis and simulations on $\mathbb{S}^2$.**

4.1. **Models.** We study both approaches A and B for $M = \mathbb{S}^2$, i.e. for a two dimensional sphere embedded in $\mathbb{R}^3$. We use spherical coordinates: let $(\theta_i)_{i\in\{1,\dots,N\}} \in [0, 2\pi]^N$, and $(\phi_i)_{i\in\{1,\dots,N\}} \in [0, \pi]^N$ such that for all $i \in \{1, \dots, N\}$,

$$x_i = (\cos\theta \sin\phi, \sin\theta \sin\phi, \cos\phi)^T.$$

Choice of influence function. We choose an influence function $\Psi(d)$ between two agents x_i and x_j so that the right-hand side of the system is continuous, the discontinuities are shown in Table 1. For Approach B, the only point in $\mathcal{CL}(x_i)$ for a given x_i is the antipodal point (this is an end point of a diameter for which x_i is the other end point.) As in the case of $\mathbb{S}^1$, for Approach B, we choose a function Ψ from a family of functions of the form Ψ^a , see equation (26) (choices of Ψ are shown in Figure 8).

Approach A. On $\mathbb{S}^2$, the derivative for system (1)-(2)-(3) with $\Psi \equiv \mathrm{Id}$ reduces to the sum of all projections onto the tangent space of agent x_i, weighted by the corresponding interaction term a_{ij}. This is rewritten as:

$$\Pi_{T_{x_i}} \sum_{j=1}^{N} a_{ij}(x_j - x_i) = \Pi_{T_{x_i}} \sum_{j=1}^{N} a_{ij}(x_j) = \sum_{j=1}^{N} a_{ij}(x_j - \langle x_j, x_i\rangle x_i) =$$
$$\sum_{j=1}^{N} a_{ij}\Big(\begin{pmatrix} \cos\theta_j \sin\phi_j \\ \sin\theta_j \sin\phi_j \\ \cos\phi_j \end{pmatrix} - \left\langle \begin{pmatrix} \cos\theta_j \sin\phi_j \\ \sin\theta_j \sin\phi_j \\ \cos\phi_j \end{pmatrix}, \begin{pmatrix} \cos\theta_i \sin\phi_i \\ \sin\theta_i \sin\phi_i \\ \cos\phi_i \end{pmatrix} \right\rangle \begin{pmatrix} \cos\theta_i \sin\phi_i \\ \sin\theta_i \sin\phi_i \\ \cos\phi_i \end{pmatrix} \Big).$$

Approach B. The geodesic distance $d_G(x_i, x_j)$ from (6) between two points x_i, and x_j on $\mathbb{S}^2$ is given by:

$$d_G(x_i, x_j) = 2 \arcsin\left(\frac{\|x_i - x_j\|}{2}\right),$$

and the direction toward x_j from x_i is

$$\nu_{ij} = \frac{x_j - \langle x_j, x_i\rangle x_i}{\|x_j - \langle x_j, x_i\rangle x_i\|},$$

where $\|\cdot\|$ is the standard norm in $\mathbb{R}^3$.

Noticing that for $\mathbb{S}^2$, Approach A with $\Psi \equiv \mathrm{Id}$ is equivalent to Approach B with $\Psi \equiv \sin$, we extend the results of Proposition 3.

Corollary 1. *Consider the dynamics given by geodesic distance (Approach B) on* $\mathbb{S}^2$, *system* (1)-(6)-(7), *and let* $\Psi \equiv \sin$. *If the interaction matrix* $A = (a_{ij})_{i,j\in\{1,\dots,N\}^2}$ *is symmetric, then*

$$\lim_{t\to\infty} E_G(t) = 0. \tag{29}$$

Proof. System (1)-(6)-(7), with $\Psi(\cdot) \equiv \sin(\cdot)$ reads:

$$\dot{x}_i = \sum_{j=1}^{N} a_{ij} \sin(d_G(x_i, x_j))\nu_{ij}. \tag{30}$$

Considering the embedding of the system in $\mathbb{R}^3$, we notice that for all $i, j \in \{1, \dots, N\}$,

$$a_{ij} \sin(d_G(x_i, x_j))\nu_{ij} = a_{ij}\Pi_{T_{x_i}M}(x_j - x_i), \tag{31}$$

thus the system is (4), and by proposition 3, $\lim_{t\to\infty} E_P(t) = 0$. Finally,

$$\lim_{t\to\infty} E_P(t) = 0 \implies \lim_{t\to\infty} \dot{x}_i = 0 \quad \text{for all } i \implies \lim_{t\to\infty} E_G(t) = 0. \tag{32}$$

□

4.2. **Simulations.** We use a fourth order Runge-Kutta scheme to approximate the trajectories. The derivative is calculated as a vector in $\mathbb{R}^3$, and then we express this vector in spherical coordinates, $\dot{\theta}t_\theta$ and $\dot{\phi}t_\phi$ where t_θ and t_ϕ are the unit vectors in the direction of the azimuth angle($\dot{\theta}$) and the polar angle($\dot{\phi}$) respectively for the ith agent. $\{t_\theta, t_\phi\}$ form an orthonormal basis for the tangent space of x_i. Using the angular derivatives avoids having to calculate the agent's trajectory in $\mathbb{R}^3$ and then project onto the sphere for every iteration which would cause significant numerical errors.

For an agent $x_i = (\theta_i, \phi_i)$ we can write t_{θ_i} and t_{ϕ_i} as

$$t_\theta = \begin{pmatrix} -\sin\theta \\ \cos\theta \\ 0 \end{pmatrix}, \qquad t_\phi = \begin{pmatrix} \cos\theta\cos\phi \\ \sin\theta\cos\phi \\ -\sin\phi \end{pmatrix}.$$

We express the derivative of an agent as

$$\dot{x}_i = \frac{\partial x_i}{\partial \theta_i}\dot{\theta} + \frac{\partial x_i}{\partial \phi_i}\dot{\phi}. \tag{33}$$

By direct computation, we get:

$$\frac{\partial x_i}{\partial \theta_i} = \begin{pmatrix} -\sin\theta_i\sin\phi_i \\ \cos\theta_i\sin\phi_i \\ 0 \end{pmatrix}, \qquad \frac{\partial x_i}{\partial \phi_i} = \begin{pmatrix} \cos\theta_i\cos\phi_i \\ \sin\theta_i\cos\phi_i \\ -\sin\phi_i \end{pmatrix}.$$

We can also express the derivative of x_i as the projection of the derivative in $\mathbb{R}^3$ with t_{θ_i} and t_{ϕ_i}

$$\dot{x}_i = \langle \dot{x}_i, t_{\theta_i}\rangle t_{\theta_i} + \langle \dot{x}_i, t_{\phi_i}\rangle t_{\phi_i}. \tag{34}$$

It follows from (33) and (34) that

$$\dot{\theta}_i = \frac{1}{\sin\phi_i}\langle \dot{x}_i, t_{\theta_i}\rangle t_{\phi_i} \quad \text{and} \quad \dot{\phi}_i = \langle \dot{x}_i, t_{\phi_i}\rangle t_{\phi_i}. \tag{35}$$

Singularities: In (35), the factor $\frac{1}{\sin\phi}$ causes a singularity around $\phi = k\pi$ for a non-negative integer k. To avoid this practical problem, before each iteration of the RK4 scheme, we identify critical agents that have a polar angle close to 0 or π ($\phi = k\pi$), for non-negative integer k; for these critical agents, we rotate all agents $\frac{\pi}{2}$ around the x-axis to calculate the derivative. This is a concern for both Approach A and Approach B.

An additional concern is singularities for agents forming consensus. In equations (3) and (7), ν_{ij} is normalized, and when agent i and agent j are very close together, dividing by d_P and d_G causes a singularity. We avoid this problem in our simulations by defining a minimum distance $d_{\min}$ between agents for the sake of the normalization term in the denominator. When $d(x_i, x_j) < d_{\min}$ then

$$\nu_{ij} = \frac{x_j - \langle x_j, x_i\rangle x_i}{d_{\min}}$$

4.3. **Examples.** We ran simulations using different choices of Ψ to see how this choice can impact the system. We show two simulations, the first uses Approach A (Figure 7); the second uses Approach B (Figure 9). In both pictures the same interaction matrix is used (given in the appendix), and we see that our choice of Ψ (Figure 8) may dramatically change the system behavior. The second example shows the effect of curvature on the system (Figure 10) for comparison to $\mathbb{T}^2$ and

$\mathbb{R}^2$ (Figure 11). Another example in the appendix shows unexpected behavior using Approach A.

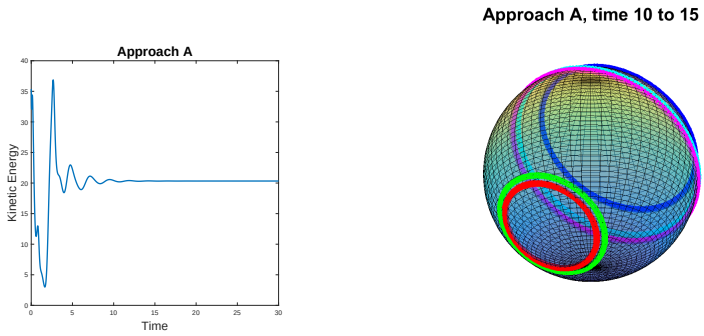

FIGURE 7. A dancing equilibrium for Approach A. The energy becomes constant in time after initial fluctuations.

Example 4.1. Five agents with a general interaction matrix A and Ψ as defined in (26) with $a \in \{\frac{\pi}{4}, \frac{\pi}{2}, \frac{3\pi}{4}\}$. The behavior of the system can change dramatically from our choice of Ψ (Figure 8), and dancing equilibria may arise from A with certain configurations, (Figure 9).

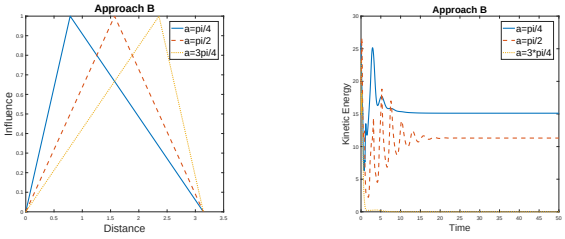

FIGURE 8. The left side shows candidates for the choice of function Ψ. The right side shows how choice of function determines the energy of the system, for the case of $a = \frac{3\pi}{4}$ the system forms an antipodal equilibrium.

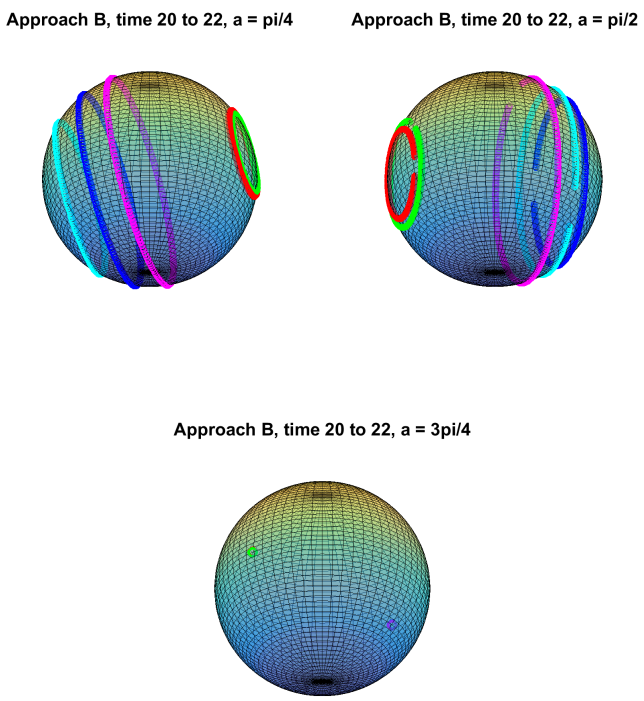

FIGURE 9. A comparison of the effect of the choice of influence function for Approach B. For $a = \frac{3\pi}{4}$ an antipodal equilibrium occurs (see Definition 2.2).

Example 4.2. To assess the influence of the curvature of $\mathbb{S}^2$ on the dynamics, observe a simple case involving 3 agents evolving according to the interaction matrix:

$$A = \begin{pmatrix} 0 & 1 & -1 \\ -1 & 0 & 1 \\ 1 & -1 & 0 \end{pmatrix} \tag{36}$$

In Section 6.2, we prove that those dynamics in $\mathbb{R}^2$ lead to periodic trajectories on a single orbit shared by all three agents, the orbit's parameters being fully determined by the initial conditions (see Theorem 6.4). However, the same dynamics on the sphere do not give rise to periodic trajectories. In sections 5.3, we also discuss the dynamics with this interactions matrix on $\mathbb{T}^2$, to assess the effect of curvature of the manifold.

5. **Analysis and simulations on $\mathbb{T}^2$.** We now study how the general dynamics given by equation (1) apply to the specific case of the torus $\mathbb{T}^2 \subset \mathbb{R}^3$. Let (e_x, e_y, e_z) denote the Euclidean basis of $\mathbb{R}^3$. Let $(R, r) \in (\mathbb{R}^+)^2$, with $R > r$. We define the manifold $\mathbb{T}^2$ as the torus obtained by rotating the circle $(x - R)^2 + z^2 = r^2$ around the z-axis. Hence $\mathbb{T}^2$ is defined by the equation $(R - \sqrt{x^2 + y^2})^2 + z^2 = r^2$. The

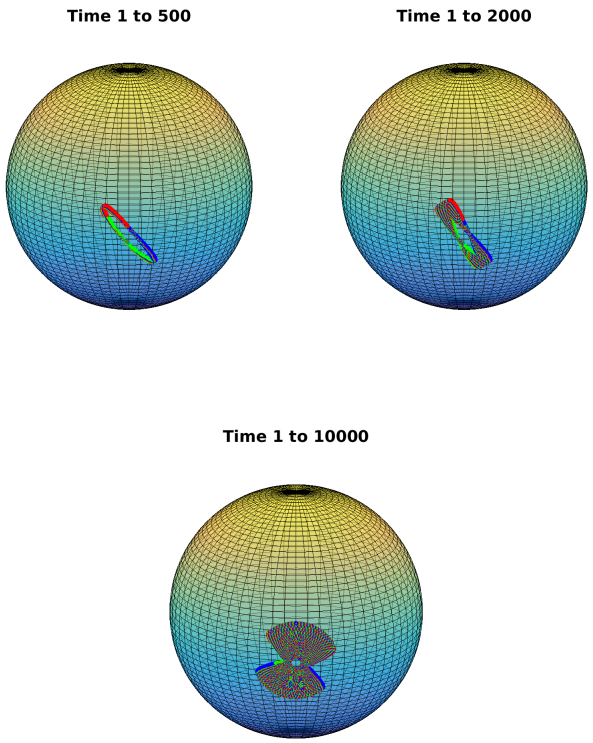

FIGURE 10. Dynamics with Approach A on $\mathbb{S}^2$, using the interactions matrix (36). If the agents' initial positions are close enough to each other, the agents with will form trajectories that remain in a neighborhood of their initial position.

parametric equations for such a torus are:

$$\begin{cases} x = (R + r\cos\theta)\cos\phi \\ y = (R + r\cos\theta)\sin\phi \\ z = r\sin\theta \end{cases} \qquad \text{for } (\phi, \theta) \in [0, 2\pi)^2.$$

The angles ϕ and θ are respectively referred to as the toroidal and poloidal angles. A set of points with the same toroidal angle is called a meridian.

5.1. **Model.** We first investigate the behavior of system (1) with Approach B (using the geodesic distance) in the case of $\mathbb{T}^2$. Unlike in the cases of $\mathbb{S}^1$ and $\mathbb{S}^2$ presented in the sections 3 and 4, there exists no simple expression for the geodesic distance between two points on the torus. In 1903, Bliss studied and classified the different kinds of geodesic lines on the standard torus [2], using elliptic functions. Gravesen et al. determined the structure of the cut loci of a torus of revolution [8].

Several challenges arise when defining Approach B on $\mathbb{T}^2$. Firstly, computing the Riemannian distance between two points is highly non-trivial. One could consider

approximating it numerically, but in the numerical discretization of equations (1)-(6)-(7), $N(N-1)/2$ geodesics would have to be computed per time-step. That would require tremendous computing power.

Secondly, assuming that one is able to efficiently compute the geodesics on $\mathbb{T}^2$, one must take into account the cut-loci of each point to ensure that the dynamics (1)-(6)-(7) are well-defined. A method to guarantee well-defined dynamics would be to use a bounded confidence model [11], where the neighborhood of influence for an agent x_i at point p is of smaller radius than the closest element in the cut locus of p. See section 2 for conditions on Ψ to make the right hand side of equation (1) continuous.

For simplicity, we thus focus on Approach A, where the dynamics are a function of the projection of each vector $x_j - x_i$ onto the tangent space at x_i. We will show that some restrictions still apply to the interaction function Ψ, but they are less restrictive and more easily determined than in Approach B.

Equations (1)-(2) reads:

$$\dot{x}_i = \sum_{j=1}^{N} a_{ij} \Psi(\|\Pi_{T_{x_i}\mathbb{T}^2}(x_j - x_i)\|)\nu_{ij}, \quad i \in \{1, \dots, N\}. \tag{37}$$

The vector ν_{ij} depends on the influence that x_j has over x_i. It is zero if $\Pi_{T_{x_i}\mathbb{T}^2}(x_j - x_i) = 0$, and it is a unit vector otherwise. Let $\mathcal{N}_i$ be the set of points that have no influence on x_i (see Table 1). Then, given $i, j \in \{1, \dots, N\}$, ν_{ij} has the following expression:

$$\nu_{ij} = \begin{cases} \frac{\Pi_{T_{x_i}\mathbb{T}^2}(x_j - x_i)}{\|\Pi_{T_{x_i}M}(x_j - x_i)\|} & \text{if } x_j \notin \mathcal{N}_i \\ 0 & \text{if } x_j \in \mathcal{N}_i. \end{cases} \tag{38}$$

Let $x_i \in \mathbb{T}^2$. We start by determining the set $\mathcal{N}_i$. For all i, we define the vectors $u_{\phi_i} = \cos\phi_i e_x + \sin\phi_i e_y$ and $u_{\theta_i} = \cos\theta_i u_{\phi_i} + \sin\theta_i e_z$, so that each agent's position vector reads: $x_i = Ru_{\phi_i} + ru_{\theta_i}$. With these notations, u_{θ_i} is the normal to the tangent space at the point x_i. A basis for the tangent space at a point $x_i(\phi_i, \theta_i)$ is given by the two tangent vectors $t_{\phi_i} = (-\sin\phi_i, \cos\phi_i, 0)$ and $t_{\theta_i} = (-\sin\theta_i\cos\phi_i, -\sin\theta_i\sin\phi_i, \cos\theta_i)$. Notice that $\langle x_i, t_{\phi_i}\rangle = 0$. Hence the condition $\Pi_{T_{x_i}\mathbb{T}^2}(x_j - x_i) = 0$ reads:

$$\begin{cases} \langle x_j, t_{\phi_i}\rangle = 0 \\ \langle x_j - x_i, t_{\theta_i}\rangle = 0. \end{cases}$$

After computations, we get:

$$\langle x_j, t_{\phi_i}\rangle = 0 \iff \sin(\phi_j - \phi_i) = 0 \iff \phi_j = \phi_i + k\pi, k \in \mathbb{Z}.$$

If $\phi_j = \phi_i$, the second condition becomes:

$$\langle x_j - x_i, t_{\theta_i}\rangle = 0 \iff \sin(\theta_j - \theta_i) = 0 \iff \theta_j = \theta_i + k\pi, k \in \mathbb{Z}.$$

If $\phi_j = \phi_i \pm \pi$, the second condition becomes:

$$\sin(\theta_i + \theta_j) = -\frac{2R}{r}\sin\theta_i.$$

Notice that this last equation only has a solution if $|\sin\theta_i| \leq \frac{r}{2R}$. The set of positions that have no influence on x_i thus comprises up to four points on the torus, depending on the values of r, R and $\sin\theta_i$. We then have: $\mathcal{N}_i = \{(\phi_i, \theta_i), (\phi_i, -\theta_i), (-\phi_i, -\theta_i -$

$\operatorname{sgn}(\sin\theta_i)\arcsin(|\frac{2R}{r}\sin\theta_i|)), (-\phi_i, \pi-\theta_i+\operatorname{sgn}(\sin\theta_i)\arcsin(|\frac{2R}{r}\sin\theta_i|))\}$. To ensure the continuity of the right-hand side of equation (37), one must impose the conditions of table 1.

We now go back to equation (37). We study the specific case where $\Psi \equiv \mathrm{Id}$, which indeed satisfies (1). Then the system becomes:

$$\dot{x}_i = \Pi_{T_{x_i}\mathbb{T}^2}\left(\sum_{j=1}^{N} a_{ij}(x_j - x_i)\right). \tag{39}$$

Hence the velocity reads:

$$\begin{aligned}\dot{x}_i &= \sum_{j=1}^{N} a_{ij}(x_j - x_i) - \langle\sum_{j=1}^{N} a_{ij}(x_j - x_i), u_{\theta_i}\rangle u_{\theta_i} \\ &= \alpha_i - \langle\alpha_i, u_{\theta_i}\rangle u_{\theta_i} - \left(\sum_{j=1}^{N} a_{ij}\right)\langle x_i, t_{\theta_i}\rangle t_{\theta_i}\end{aligned}$$

where $\alpha_i := \sum_{j=1}^{N} a_{ij}x_j$ is the sum of the influences of all agents on agent i. Notice that with the same notation, the system does not reduce to the simple form $\dot{x}_i = \alpha_i - \langle\alpha_i, x_i\rangle x_i$ for the same dynamics on the sphere (see [3]). This is due to the fact that on the torus, the position vector x_i does not define the normal to the tangent space at x_i, unlike in the cases of $\mathbb{S}^1$ and $\mathbb{S}^2$.

The velocity of each agent is given by:

$$\dot{x}_i = \begin{pmatrix} -\dot{\phi}_i\sin\phi_i(R + r\cos\theta_i) - r\dot{\theta}_i\sin\theta_i\cos\phi_i \\ \dot{\phi}_i\cos\phi_i(R + r\cos\theta_i) - r\dot{\theta}_i\sin\theta_i\sin\phi_i \\ r\dot{\theta}_i\cos\theta_i \end{pmatrix} = \dot{\phi}_i(R + r\cos\theta_i)t_{\phi_i} + r\dot{\theta}_i t_{\theta_i}. \tag{40}$$

From (39) and (40) we get the angular velocities:

$$\begin{cases} \dot{\phi}_i = \frac{1}{(R+r\cos\theta_i)}\langle\sum_{j=1}^{N} a_{ij}(x_j - x_i), t_{\phi_i}\rangle \\ \dot{\theta}_i = \frac{1}{r}\langle\sum_{j=1}^{N} a_{ij}(x_j - x_i), t_{\theta_i}\rangle. \end{cases} \tag{41}$$

Notice that unlike in the case of $\mathbb{S}^2$, see equation (35), here the derivatives $\dot{\phi}_i$ and $\dot{\theta}_i$ are not singular. This makes numerical simulations straightforward, not requiring the approximations described in Section 4.2.

5.2. **Properties.** We now analyze the dynamics (1)-(2)-(3) on $\mathbb{T}^2$. We identify families of initial conditions that trivialize the dynamics.

Proposition 4. *Consider the dynamics (1)-(2)-(3) on $M = \mathbb{T}^2$. Let $P_z := \{(x, y, z) \in \mathbb{R}^3 \mid z = 0\}$. Let $x_i(t)$ be the position of the $i$the agent at time t. If for all $i \in \{1, \dots, N\}$, $x_i(0) \in \mathbb{T}^2 \cap P_z$, then for all $t \geq 0$, for all $i \in \{1, \dots, N\}$, $x_i(t) \in \mathbb{T}^2 \cap P_z$.*

Proof. Suppose that for all $i \in \{1, \dots, N\}$, $x_i(0) \in \mathbb{T}^2 \cap P_z$. Then for all $i \in \{1, \dots, N\}$, $\theta_i(0) = 0$ or $\theta_i(0) = \pi$. Hence, for all $i, j \in \{1, \dots, N\}$,

$$t_{\theta_i}(0) = \begin{pmatrix} 0 \\ 0 \\ \pm\pi \end{pmatrix} \text{ and } x_j(0) - x_i(0) = \begin{pmatrix} (R + r\cos\theta_j)\cos\phi_j - (R + r\cos\theta_i)\cos\phi_i \\ (R + r\cos\theta_j)\sin\phi_j - (R + r\cos\theta_i)\sin\phi_i \\ 0 \end{pmatrix}$$

From equation (41) we get: for all $i \in \{1, \dots, N\}$, $\dot{\theta}_i = 0$. By uniqueness of solution, for all $i \in \{1, \dots, N\}$, $\theta_i(t) = \theta_i(0)$. All the initial velocities belong to the plane P_z. Hence all agents remain on P_z at all time. □

Remark 5. As a consequence of Proposition 4, if all agents are initially in $\mathbb{T}^2 \cap P_z$, all agents initially on the bigger circle $\theta = 0$ remain on the major circle at all time and all agents on the minor circle $\theta = \pi$ remain on the minor circle at all time. In particular, if all agents are initially all on the same circle (i.e. for all $i \in \{1, \dots, N\}$, $\theta_i = 0$ or for all $i \in \{1, \dots, N\}$, $\theta_i = \pi$), then the torus dynamics simplify to the dynamics on $\mathbb{S}^1$ given by (22) or (23).

Proposition 5. *Consider the dynamics* (1)-(2)-(3) *on* $M = \mathbb{T}^2$. *Let* $\tilde{\phi} \in [0, 2\pi]$ *and let* $P_{\tilde{\phi}} := \{(x, y, z) \in \mathbb{R}^3 \mid y = \tan(\tilde{\phi})x\}$. *If for all* $i \in \{1, \dots, N\}$, $x_i(0) \in \mathbb{T}^2 \cap P_{\tilde{\phi}}$, *then for all* $t \geq 0$, *for all* $i \in \{1, \dots, N\}$, $x_i(t) \in \mathbb{T}^2 \cap P_{\tilde{\phi}}$.

Proof. Suppose without loss of generality that $\bar{\phi} = 0$. Similarly to the proof for Proposition 4, we can show that for all $i \in \{1, \dots, N\}$, $\dot{\phi}_i(0) = 0$. By uniqueness of solution, for all $i \in \{1, \dots, N\}$, $\phi_i(t) = \phi_i(0)$. Hence all agents remain in $P_{\tilde{\phi}}$ at all time. □

Remark 6. As a consequence of Proposition 5, if all agents are initially in $\mathbb{T}^2 \cap P_{\bar{\phi}}$, all agents initially on the circle $\phi = \bar{\phi}$ remain on that circle at all time and all agents on the circle $\phi = -\bar{\phi}$ remain on that circle at all time. In particular, if all agents are initially all on the same circle (i.e. for all $i \in \{1, \dots, N\}$, $\phi_i = \bar{\phi}$ or for all $i \in \{1, \dots, N\}$, $\phi_i = -\bar{\phi}$), then the torus dynamics simplify to the dynamics on $\mathbb{S}^1$ given by (22) or (23).

5.3. **Simulations.** To assess the influence of the curvature of the manifold on the dynamics, we compare a simple case involving 3 agents evolving according to the interaction matrix given in equation (36). As in the case of $\mathbb{S}^2$, the dynamics on the torus do not give rise to periodic trajectories (as opposed to the dynamics in $\mathbb{R}^2$, see Theorem 6.4). Instead, since $\mathbb{T}^2$ can locally be identified with $\mathbb{R}^2$, if the initial mutual distances are small enough, the dynamics resemble those in $\mathbb{R}^2$. More specifically, the trajectories are quasi-periodic with a gradual shift of the center of mass (see Figure 11). However, if the initial distances between agents are large, the geometry and curvature of the torus changes radically the behavior of the system.

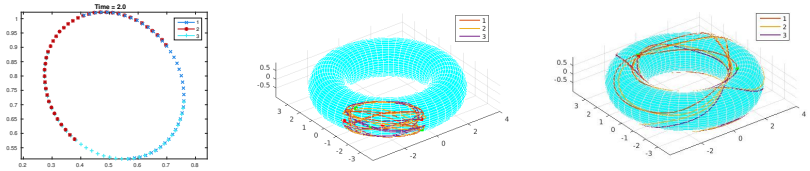

FIGURE 11. Trajectories of three agents interacting according to the matrix A given in (36). Left: Dynamics in $\mathbb{R}^2$, with periodic trajectories on a unique orbit. Center: Dynamics on $M = \mathbb{T}^2$ with small initial mutual distances. Right: Dynamics on $M = \mathbb{T}^2$ with large initial distances.

6. **Social choreographies.** As seen in Sections 3 and 5.3, when the interaction matrix A satisfies certain properties, for instance given by (28) on $\mathbb{S}^1$ or by (36) in $\mathbb{R}^2$, then the trajectories exhibit special properties of symmetry or periodicity. In [3], configurations on $\mathbb{S}^2$ in which all mutual distances between agents remain constant were named *dancing equilibrium*.

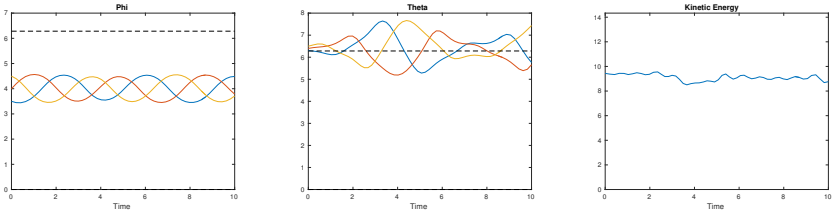

FIGURE 12. Evolutions of the coordinates of the three agents evolving on $\mathbb{T}^2$ with interaction matrix A from equation (36), with small initial mutual distances. Left: Evolution of ϕ. Center: Evolution of θ. Right: Evolution of the kinetic energy.

In this section, we investigate systems with similar properties of periodicity or symmetry. We use the term *social choreography*, drawing a parallel with the well-known "n-body choreographies" discovered by Moore [13, 14] in the context of point masses subject to gravitational forces. In the n-body problem, the interaction potentials between masses are predetermined, as they depend exclusively on the masses and distances between agents. Hence the conditions for a n-body choreography to occur only depend on the initial state of the system. In the case of social choreography, there are more degrees of freedom, as we design the interaction matrix as well as to set the initial conditions.

We study sufficient conditions on the interaction matrices for the trajectories of the system to be periodic or symmetric by focusing on the Euclidean space $\mathbb{R}^2$, with the specific choice of interaction potential $\Psi \equiv \mathrm{Id}$. A future direction of this paper can consist in extending these results to general Riemannian manifolds. In $\mathbb{R}^2$ and with $\Psi \equiv \mathrm{Id}$, both approaches A and B are equivalent and the system simply reads as:

$$\text{for all } i \in \{1, \dots, N\}, \quad \dot{x}_i = \sum_{j=1}^{N} a_{ij}(x_j - x_i). \tag{42}$$

We define the kinetic energy $E = E_G = E_P$ as in Definition 2.3:

$$E(t) := \frac{1}{2} \sum_{i=1}^{N} \|\dot{x}_i(t)\|^2. \tag{43}$$

A simple case of social choreography is that of a system with periodic trajectories, which we define as follows:

Definition 6.1. Let $(x_i)_{i=1\dots N}$ be a solution of (42). We refer to the system as having **periodic trajectories** if there exists $\tau > 0$ such that

$$\text{for all } i \in \{1, ..., N\}, \text{ for all } t > 0, \quad x_i(t + \tau) = x_i(t).$$

We will examine possible periodic behaviors of the system in sections 6.2, 6.3 and 6.4.

6.1. **Rotationally invariant system.** We now give sufficient conditions on the interaction matrix and on the initial conditions for the system to be invariant by rotation.

Theorem 6.2. *Let $k \in \mathbb{N}$ such that k divides N. Let $P_k = \begin{pmatrix} 0 & I_{N-k} \\ I_k & 0 \end{pmatrix}$ be the matrix of change of basis from $(e_1, \dots, e_N)$ to $(e_k, \dots, e_N, e_1, \dots, e_{k-1})$. Let $R(\theta)$*

denote the rotation matrix in $\mathbb{R}^2$ *for the angle* $\theta \in [0, 2\pi)$. *Suppose that initially, the system is invariant by rotation of angle* $\frac{2k\pi}{N}$, *that is:*

$$\text{for all } i \in \{1, \dots, N\}, \quad R(\frac{2k\pi}{N})x_i(0) = \begin{cases} x_{i+k}(0) & \text{if } i+k \leq N \\ x_{i+k-N}(0) & \text{if } i+k > N \end{cases}.$$

Suppose that the interaction matrix A *is invariant by change of basis, i.e.* $P_k^{-1}AP_k = A$. *Then the system remains invariant by rotation of angle* $\frac{2k\pi}{N}$ *at all time:*

$$\text{for all } t > 0, \quad \text{for all } i \in \{1, \dots, N\}, \quad R(\frac{2k\pi}{N})x_i(t) = \begin{cases} x_{i+k}(t) & \text{if } i+k \leq N \\ x_{i+k-N}(t) & \text{if } i+k > N \end{cases}.$$

Proof. Let $A \in \mathcal{M}^N(\mathbb{R})$ be the interaction matrix, i.e. $A = (a_{ij})_{i,j=1,\dots N}$, and define $D = \text{diag}(\sum_j a_{ij})$. Let $x = (x_1, \dots, x_N)$ denote the set of all x_i's. It is a vector of length N with entries in $\mathbb{R}^2$. Let $X \in \mathcal{M}^{N\times 2}(\mathbb{R})$ denote the corresponding matrix of $\mathbb{R}^{N\times 2}$ such that for all $i \in \{1, \dots, N\}$, for all $j \in \{1, 2\}$, X_{ij} is the j-th coordinate of x_i. With these notations, $\dot{X} = \tilde{A}X$, where $\tilde{A} = A - D$. We denote by $(e_1, \dots, e_N)$ the canonical orthonormal basis of $(\mathbb{R})^N$ such that $X = \sum_{i=1}^N e_i x_i^T$.

From the definition of the matrix X, the condition

$$\text{for all } i \in \{1, \dots, N\}, \quad R(\frac{2k\pi}{N})x_i(0) = \begin{cases} x_{i+k}(0) & \text{if } i+k \leq N \\ x_{i+k-N}(0) & \text{if } i+k > N \end{cases}$$

can be rewritten as: $P_kX(0) = (R(\frac{2k\pi}{N})X(0)^T)^T$. Let $Y := P_kX$ and $Z := (R(\frac{2k\pi}{N})X^T)^T$. From the theorem's hypotheses, $Y(0) = Z(0)$. Let us show that Y and Z have the same evolution. One can easily prove that $P_k^{-1}\tilde{A}P_k$ if and only if $P_k^{-1}AP_k$. Then notice that

$$\dot{X} = \tilde{A}X = P_k^{-1}\tilde{A}P_kX.$$

From that we compute:

$$\dot{Y} = P_k\dot{X} = P_k(P_k^{-1}\tilde{A}P_kX) = \tilde{A}P_kX = \tilde{A}Y.$$

Similarly,

$$\dot{Z} = (R(\frac{2k\pi}{N})\dot{X}^T)^T = (R(\frac{2k\pi}{N})(\tilde{A}X)^T)^T = (R(\frac{2k\pi}{N})X^T\tilde{A}^T)^T = \tilde{A}Z.$$

Since Y and Z satisfy the same differential equation and $Y(0) = Z(0)$, then $Y(t) = Z(t)$ for all $t \geq 0$. This implies that at all time,

$$\text{for all } i \in \{1, \dots, N\}, \quad R(\frac{2k\pi}{N})x_i(t) = \begin{cases} x_{i+k}(t) & \text{if } i+k \leq N \\ x_{i+k-N}(t) & \text{if } i+k > N \end{cases}.$$

□

6.2. **Unique orbit.** Another example of social choreography is that of a system in which all agents share one unique orbit. Such choreographies have been discovered in the context of the n-body problem, for instance the "figure 8" orbit for three equal masses [13].

Definition 6.3. Let $(x_i)_{i=1\dots N}$ be a solution of (42). We say that the system has a **unique orbit** if the orbits of all points are identical, i.e.

$$\text{for all } i, j \in \{1, ..., N\}, \quad \{z \in M | \exists t > 0,\ x_i(t) = z\} = \{z \in M | \exists t > 0,\ x_j(t) = z\}.$$

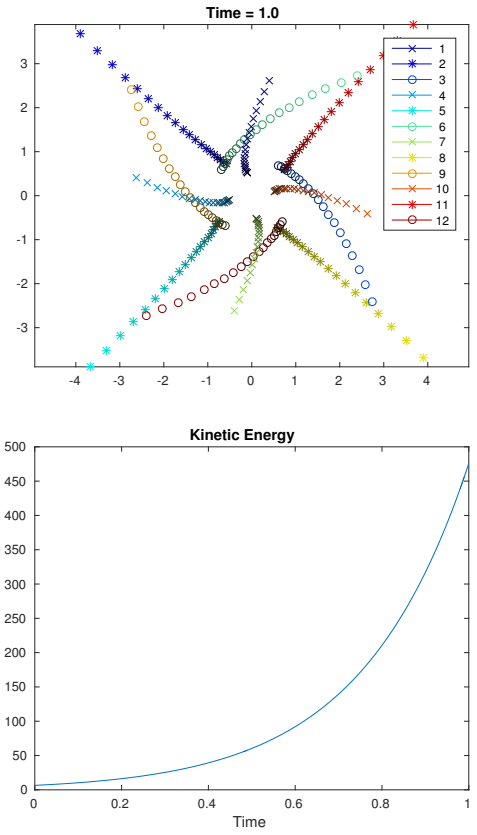

FIGURE 13. Left: Evolution of 12 agents with the conditions of Theorem 6.2, with $k = 3$, resulting in diverging trajectories. Dark to light color scale indicates earlier to later time. Right: corresponding exploding kinetic energy. The interaction matrix A and the initial positions were generated according to a random algorithm, with the conditions of Theorem 6.2.

To illustrate Theorem 6.2, we study the evolution of N agents initially positioned at regular intervals on a circle, with an interaction matrix and initial conditions given by:

$$A = \begin{pmatrix} 0 & 1 & 0 & \dots & 0 & -1 \\ -1 & 0 & \ddots & \ddots & \ddots & 0 \\ 0 & \ddots & \ddots & \ddots & \ddots & \vdots \\ \vdots & \ddots & \ddots & \ddots & \ddots & 0 \\ 0 & \ddots & \ddots & \ddots & \ddots & 1 \\ 1 & 0 & \dots & 0 & -1 & 0 \end{pmatrix} \tag{44}$$

$$\text{and for all } i \in \{1, \dots, N\}, \quad x_i(0) = \begin{pmatrix} \cos(\frac{2i\pi}{N}) \\ \sin(\frac{2i\pi}{N}) \end{pmatrix}.$$

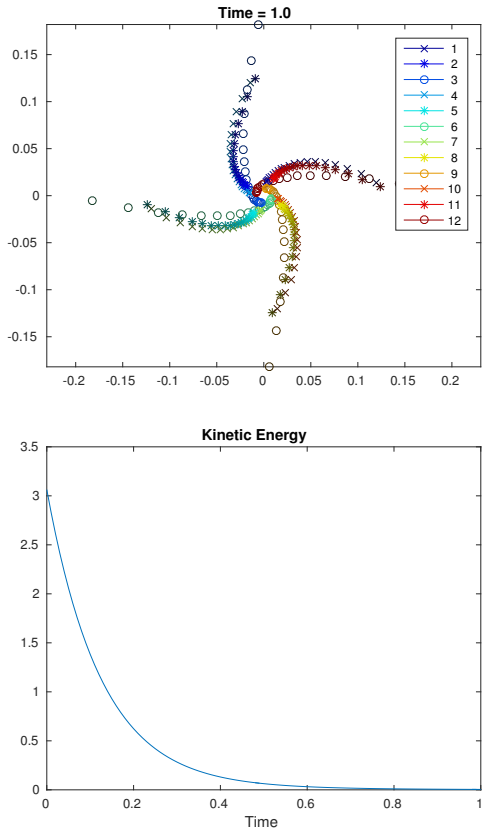

FIGURE 14. Left: Evolution of 12 agents with the conditions of Theorem 6.2, with $k = 3$, resulting in convergence to consensus. Dark to light color scale indicates earlier to later time. Right: corresponding kinetic energy converging to zero. The interaction matrix A and the initial positions were generated according to a random algorithm, with the conditions of Theorem 6.2.

Notice that $\tilde{A} = A$, and the system satisfies the conditions of Theorem 6.2 with $k = 1$. Hence for all $i \in \{1, \dots, N-1\}$, $R(\frac{2\pi}{N})x_i(t) = x_{i+1}(t)$ and $R(\frac{2\pi}{N})x_N(t) = x_1(t)$. The $2N$-dimensional system then reduces to a 2-dimensional one for the two coordinates x_{11} and x_{12} of x_1, and all the other variables can be recovered by rotation of x_1:

$$\dot{x}_1 = x_2 - x_N = R(\frac{2\pi}{N})x_1 - R(-\frac{2\pi}{N})x_1.$$

This can be written as:

$$\begin{pmatrix} \dot{x}_{11} \\ \dot{x}_{12} \end{pmatrix} = \begin{pmatrix} 0 & -2\sin(\frac{2\pi}{N}) \\ 2\sin(\frac{2\pi}{N}) & 0 \end{pmatrix} \begin{pmatrix} x_{11} \\ x_{12} \end{pmatrix}.$$

Solving this linear system yields:

$$\begin{cases} x_{11}(t) = x_{11}(0)\cos(2\sin(\frac{2\pi}{N})t) - x_{12}(0)\sin(2\sin(\frac{2\pi}{N})t) = \cos(2\sin(\frac{2\pi}{N})t) \\ x_{12}(t) = x_{11}(0)\sin(2\sin(\frac{2\pi}{N})t) + x_{12}(0)\cos(2\sin(\frac{2\pi}{N})t) = \sin(2\sin(\frac{2\pi}{N})t) \end{cases}.$$

This proves that all agents share one common circular orbit, and their trajectories are periodic of period $2\pi(2\sin(\frac{2\pi}{N}))^{-1}$. Figure 15 provides a numerical illustration of this behavior, with 10 agents initially positioned at regular intervals on the unit circle.

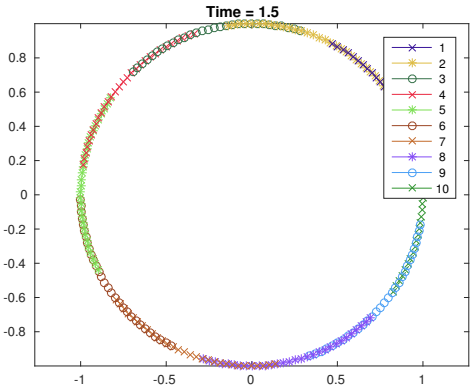

FIGURE 15. Evolution of 10 agents with initial conditions and interaction matrix given in (44). The agents have periodic trajectories along one shared circular orbit.

Another interesting example is that of 3 agents interacting according to the interaction matrix given previously, which, reduced to $N = 3$, gives:

$$A = \begin{pmatrix} 0 & 1 & -1 \\ -1 & 0 & 1 \\ 1 & -1 & 0 \end{pmatrix}. \tag{45}$$

Theorem 6.4. *Let $N = 3$. Consider the system (42) with interaction matrix given by (45). Then there exists a unique orbit shared by all agents, and all three trajectories are periodic.*

Proof. The x and y-coordinates of the systems are decoupled, so that the 6-dimensional system can be reduced to two 3-dimensional ones. Notice that $\tilde{A} = A$. Then for each coordinate $j \in \{1, 2\}$, the system reads:

$$\begin{pmatrix} x_{1j} \\ x_{2j} \\ x_{3j} \end{pmatrix}(t) = \exp(tA) \begin{pmatrix} x^0_{1j} \\ x^0_{2j} \\ x^0_{3j} \end{pmatrix}$$

with

$$e^{tA} = \frac{1}{3}\begin{pmatrix} 1+2\cos(\sqrt{3}t) & 1-\cos(\sqrt{3}t)+\sqrt{3}\sin(\sqrt{3}t) & 1-\cos(\sqrt{3}t)-\sqrt{3}\sin(\sqrt{3}t) \\ 1-\cos(\sqrt{3}t)-\sqrt{3}\sin(\sqrt{3}t) & 1+2\cos(\sqrt{3}t) & 1-\cos(\sqrt{3}t)+\sqrt{3}\sin(\sqrt{3}t) \\ 1-\cos(\sqrt{3}t)+\sqrt{3}\sin(\sqrt{3}t) & 1-\cos(\sqrt{3}t)-\sqrt{3}\sin(\sqrt{3}t) & 1+2\cos(\sqrt{3}t) \end{pmatrix}.$$

Due to the special structure of e^{tA}, this can be rewritten as:

$$\begin{pmatrix} x_{1j} \\ x_{2j} \\ x_{3j} \end{pmatrix}(t) = \frac{1}{3}\begin{pmatrix} x^0_{1j} & x^0_{2j} & x^0_{3j} \\ x^0_{2j} & x^0_{3j} & x^0_{1j} \\ x^0_{3j} & x^0_{1j} & x^0_{2j} \end{pmatrix} \begin{pmatrix} 1+2\cos(\sqrt{3}t) \\ 1-\cos(\sqrt{3}t)+\sqrt{3}\sin(\sqrt{3}t) \\ 1-\cos(\sqrt{3}t)-\sqrt{3}\sin(\sqrt{3}t) \end{pmatrix}.$$

This shows that all three trajectories are periodic, or period $\frac{2\pi}{\sqrt{3}}$. One can compute the positions of each agent after a third of a period and notice that:

$$\begin{pmatrix} x_{1j} \\ x_{2j} \\ x_{3j} \end{pmatrix} (t + \frac{2\pi}{3\sqrt{3}})$$

$$= \frac{1}{3} \begin{pmatrix} x^0_{1j} & x^0_{2j} & x^0_{3j} \\ x^0_{2j} & x^0_{3j} & x^0_{1j} \\ x^0_{3j} & x^0_{1j} & x^0_{2j} \end{pmatrix} \begin{pmatrix} 1 - \cos(\sqrt{3}t) - \sqrt{3}\sin(\sqrt{3}t) \\ 1 + 2\cos(\sqrt{3}t) \\ 1 - \cos(\sqrt{3}t) + \sqrt{3}\sin(\sqrt{3}t) \end{pmatrix} = \begin{pmatrix} x_{2j} \\ x_{3j} \\ x_{1j} \end{pmatrix} (t).$$

This shows that there is one unique shared orbit. □

6.3. **Coupled periodic trajectories.** Other conditions on the interaction matrix A give rise to different kinds of periodic behaviors. Here we provide sufficient conditions for the system to exhibit periodic trajectories, such that each orbit is shared by two agents.

Theorem 6.5 (Coupled periodic trajectories)**.** *Let N be even. Suppose that initially, the system is invariant by rotation of angle $\frac{4\pi}{N}$, that is:*

$$\text{for all } i \in \{1, \dots, N\}, \quad R(\frac{4\pi}{N})x_i(0) = \begin{cases} x_{i+2}(0) & \text{if } i+2 \leq N \\ x_{i+2-N}(0) & \text{if } i+2 > N \end{cases}.$$

Let $a, b > 0$ and let

$$A = \begin{pmatrix} 0 & a & 0 & \dots & 0 & -b \\ -a & 0 & b & \ddots & \ddots & 0 \\ 0 & -b & \ddots & a & \ddots & \vdots \\ \vdots & \ddots & \ddots & \ddots & \ddots & 0 \\ 0 & \ddots & \ddots & \ddots & \ddots & a \\ b & 0 & \dots & 0 & -a & 0 \end{pmatrix}. \tag{46}$$

Then the system is periodic of period $\tau = \frac{\pi}{\sqrt{ab}\sin(2\pi/N)}$. Furthermore, if N is divisible by 4, opposite agents share orbits two by two, i.e.:

$$\text{for all } t > 0, \text{ for all } i \in \{1, \dots, \frac{N}{2}\}, x_i(t+\tau) = x_{i+\frac{N}{2}}(t),$$

and the kinetic energy is periodic with period $\tau/2$.

Proof. First remark that the system satisfies the hypotheses of Theorem 6.2, so

$$\text{for all } t > 0, \quad \text{for all } i \in \{1, \dots, N\}, \quad R(\frac{4\pi}{N})x_i(t) = \begin{cases} x_{i+2}(t) & \text{if } i+2 \leq N \\ x_{i+2-N}(t) & \text{if } i+2 > N \end{cases}.$$

Hence the system is entirely known from the positions of the first two agents, since all others can be obtained by simple rotations. We show that this $2N$-dimensional problem can be rewritten as a 4-dimensional one. Indeed, using the fact that $x_N = R(-4\pi/N)x_2$ and $x_3 = R(4\pi/N)x_1$, the system

$$\begin{cases} \dot{x}_1 = a(x_2 - x_1) - b(x_N - x_1) \\ \dot{x}_2 = b(x_3 - x_2) - a(x_1 - x_2) \end{cases}$$

becomes:

$$\begin{cases} \dot{x}_1 = \begin{pmatrix} \dot{x}_{11} \\ \dot{x}_{12} \end{pmatrix} = a\left[\begin{pmatrix} x_{21} \\ x_{22} \end{pmatrix} - \begin{pmatrix} x_{11} \\ x_{12} \end{pmatrix}\right] - b\left[\begin{pmatrix} \cos(\frac{4\pi}{N}) & \sin(\frac{4\pi}{N}) \\ -\sin(\frac{4\pi}{N}) & \cos(\frac{4\pi}{N}) \end{pmatrix}\begin{pmatrix} x_{21} \\ x_{22} \end{pmatrix} - \begin{pmatrix} x_{11} \\ x_{12} \end{pmatrix}\right] \\ \dot{x}_2 = \begin{pmatrix} \dot{x}_{21} \\ \dot{x}_{22} \end{pmatrix} = b\left[\begin{pmatrix} \cos(\frac{4\pi}{N}) & -\sin(\frac{4\pi}{N}) \\ \sin(\frac{4\pi}{N}) & \cos(\frac{4\pi}{N}) \end{pmatrix}\begin{pmatrix} x_{11} \\ x_{12} \end{pmatrix} - \begin{pmatrix} x_{21} \\ x_{22} \end{pmatrix}\right] - a\left[\begin{pmatrix} x_{11} \\ x_{12} \end{pmatrix} - \begin{pmatrix} x_{21} \\ x_{22} \end{pmatrix}\right] \end{cases}.$$

This can be rewritten in matrix form as:

$$\begin{pmatrix} \dot{x}_{11} \\ \dot{x}_{12} \\ \dot{x}_{21} \\ \dot{x}_{22} \end{pmatrix} = A_4 \begin{pmatrix} x_{11} \\ x_{12} \\ x_{21} \\ x_{22} \end{pmatrix} \tag{47}$$

where

$$A_4 := \begin{pmatrix} -a+b & 0 & a-b\cos(\frac{4\pi}{N}) & -b\sin(\frac{4\pi}{N}) \\ 0 & -a+b & b\sin(\frac{4\pi}{N}) & a-b\cos(\frac{4\pi}{N}) \\ -a+b\cos(\frac{4\pi}{N}) & -b\sin(\frac{4\pi}{N}) & a-b & 0 \\ b\sin(\frac{4\pi}{N}) & -a+b\cos(\frac{4\pi}{N}) & 0 & a-b \end{pmatrix}\begin{pmatrix} x_{11} \\ x_{12} \\ x_{21} \\ x_{22} \end{pmatrix}.$$

One can easily show that this reduced interaction matrix A_4 has two purely imaginary conjugate eigenvalues, $i\lambda$ and $-i\lambda$, each of multiplicity 2, where $\lambda = 2\sqrt{ab}\sin(\frac{2\pi}{N})$. Hence the solution of the system (47) can be written as a weighted sum of the functions $t \mapsto \cos(\lambda t)$ and $t \mapsto \sin(\lambda t)$. This implies that the system is periodic, of period

$$\tau = \frac{2\pi}{\lambda} = \frac{\pi}{\sqrt{ab}\sin(\frac{2\pi}{N})}.$$

Furthermore, if N is divisible by 4, according to Theorem 6.2, $x_{\frac{N}{2}+1} = -x_1$ and $x_{\frac{N}{2}+2} = -x_2$. This implies that for all $t > 0$, $x_1(t+\tau) = -x_1(t) = x_{\frac{N}{2}+1}(t)$ and $x_2(t+\tau) = -x_2(t) = x_{\frac{N}{2}+2}(t)$, so the agents x_1 and $x_{\frac{N}{2}+1}$ share an orbit, as well as all pairs of agents x_i and $x_{\frac{N}{2}+i}$ for $i \in \{1, \dots, \frac{N}{2}\}$.

As a consequence, the kinetic energy is periodic, of period $\tau_E = \tau = \pi/(\sqrt{ab}\sin(\frac{2\pi}{N}))$. If N is divisible by 4, every half period, the system is rotated by an angle π, so the kinetic energy is periodic with period $\tau_E = \tau/2$. □

Remark 7. Notice that the agents sharing orbits do not interact with one another, as shown in Figure 16.

An example of such a choreography is given in Figure 17.

Remark 8. As a slight generalization, we provide numerical simulations illustrating a similar behavior, but with slightly different conditions: the periodic evolution of 9 agents on three distinct orbits shared three by three, see figures 18 and 19.

6.4. **Helical trajectories.** In sections 6.2 and 6.3, we provided conditions for the trajectories of the system to be periodic. Here, we explore further the notion of periodicity by studying systems with drift, displaying helical trajectories but periodic kinetic energy.

Definition 6.6. Let $(x_i)_{i=1\dots N}$ be a solution of (42). We call the corresponding trajectories **helical trajectories** if there exists $v \in \mathbb{R}^2$ and $\tau \in \mathbb{R}^*$ such that

$$\text{for all } i \in \{1, \dots, N\}, \text{ for all } t > 0, \quad x_i(t+\tau) = x_i(t) + \tau v.$$

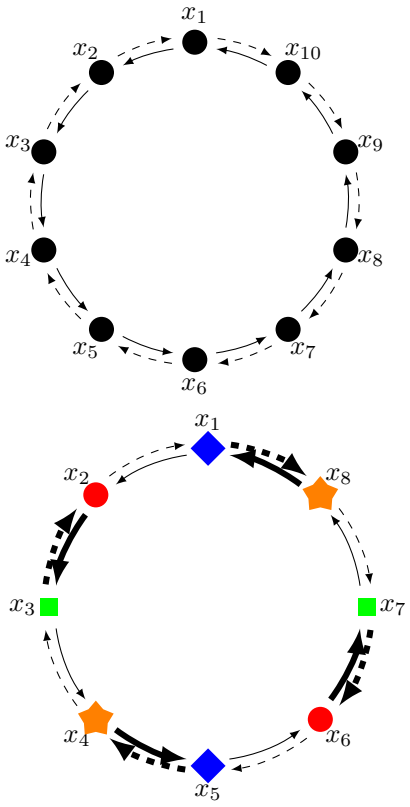

FIGURE 16. Left: Directed graph corresponding to the matrix A given in (44). Full arrows represent positive coefficients ($a_{ij} > 0$) while dashed ones represent negative coefficients ($a_{ij} < 0$). Right: Weighted directed graph corresponding to the matrix A given in (46). Thin arrows represent the weighted edges $|a_{ij}| = a$ while bold ones represent the weight $|a_{ij}| = b$. Nodes with the same color and symbol share orbits but are not directly connected in the graph.

Notice that this definition generalizes the notion of periodic trajectories recalled in Definition 6.1, which corresponds to the case $v = 0$. When $v \neq 0$, the system has a drift term, meaning that the relative positions between agents remain periodic but their absolute positions evolve in space.

Theorem 6.7. *Sufficient conditions for helical trajectories. Let $N = 4$. Let $(a, b, c, d) \in (\mathbb{R}^+)^4$ such that the interaction matrix reads*

$$A = \begin{pmatrix} 0 & a & 0 & -d \\ -a & 0 & b & 0 \\ 0 & -b & 0 & c \\ d & 0 & -c & 0 \end{pmatrix}. \tag{48}$$

Then the system exhibits helical trajectories.

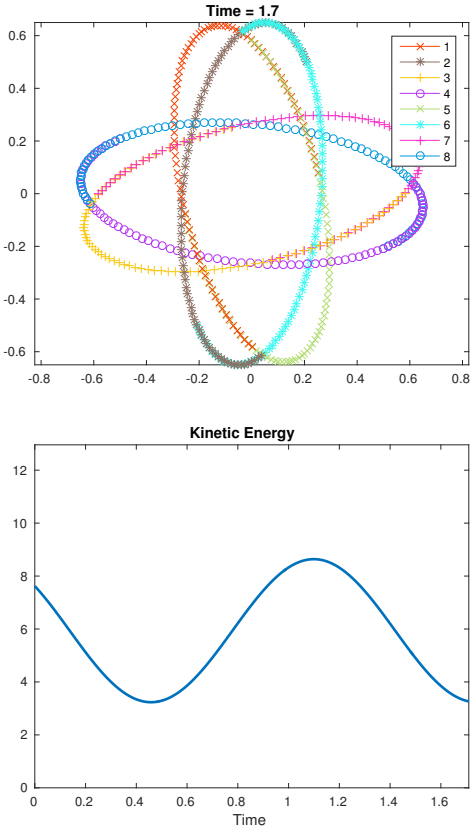

FIGURE 17. Left: Periodic trajectories of 8 agents sharing orbits two by two, in the situation of Theorem 6.5. Matrix A from (46) was constructed with $(a, b) = (1, 3)$. The initial positions $x_1(0)$ and $x_2(0)$ were randomly generated and the other 6 were obtained by rotation. The period is $\tau = 2\pi/\sqrt{6}$. Right: Corresponding kinetic energy, of period $\tau/2$.

Proof. First notice that the first and second components x_{i1} and x_{i2} of the i-th agent's position are decoupled, so that the system in matrix form reads

$$\dot{x}^j = \begin{pmatrix} \dot{x}_{1j} \\ \dot{x}_{2j} \\ \dot{x}_{3j} \\ \dot{x}_{4j} \end{pmatrix} = \begin{pmatrix} d-a & a & 0 & -d \\ -a & a-b & b & 0 \\ 0 & -b & b-c & c \\ d & 0 & -c & c-d \end{pmatrix} \begin{pmatrix} x_{1j} \\ x_{2j} \\ x_{3j} \\ x_{4j} \end{pmatrix} := \tilde{A} \begin{pmatrix} x_{1j} \\ x_{2j} \\ x_{3j} \\ x_{4j} \end{pmatrix}, \text{ for } j \in \{1, 2\}. \tag{49}$$

Hence the projections of x on the first and second axes solve the same differential equation. The matrix $\tilde{A}$ has three distinct eigenvalues:

$$\lambda_1 = 0, \quad \lambda_2 = i\sqrt{(a+c)(b+d)} \quad \text{and} \quad \lambda_3 = -i\sqrt{(a+c)(b+d)}.$$

There is one eigenvector associated with λ_1: $v_1 := (1, 1, 1, 1)^T$. One can show that the vectors $x(t) = v_1$ and $x(t) = v_1 t + \nu$ are both solutions of System (49), where,

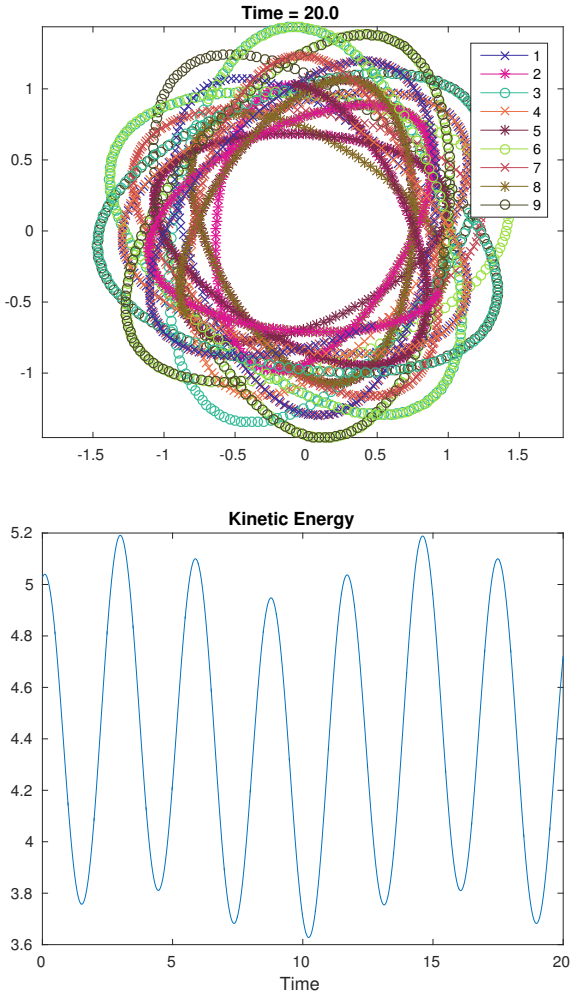

FIGURE 18. Left: evolution of 9 agents with periodic trajectories, each orbit shared by 3 agents. Right: periodic kinetic energy.

denoting $\Delta := bcd - abc + abd - acd$,

$$\nu := \frac{1}{\Delta}(ab + bc + \Delta, ab - cd + \Delta, ab + ad + \Delta, \Delta)^T.$$

Let v_2 denote the eigenvector associated with λ_2 and let v_2^R and v_2^I denote respectively its real and imaginary components, i.e. $v_2 := v_2^R + iv_2^I$. Then the solution of System (49) can be written as:

$$\begin{aligned} x^j(t) = C_1^j v_1 + C_2^j(v_1 t + \nu) + C_3^j \left[v_2^R \cos(\lambda_2 t) - v_2^I \sin(\lambda_2 t)\right] \\ + C_4^j \left[v_2^R \sin(\lambda_2 t) + v_2^I \cos(\lambda_2 t)\right] \end{aligned}$$

where $(C_1, C_2, C_3, C_4) \in \mathbb{R}^4$ are constants depending on the initial conditions. Let $\tau = \frac{2\pi}{\lambda_2}$. Then for all $t > 0$, for all $i \in \{1, \ldots, 4\}$, for all $j \in \{1, 2\}$, $x_{ij}(t + \tau) =$

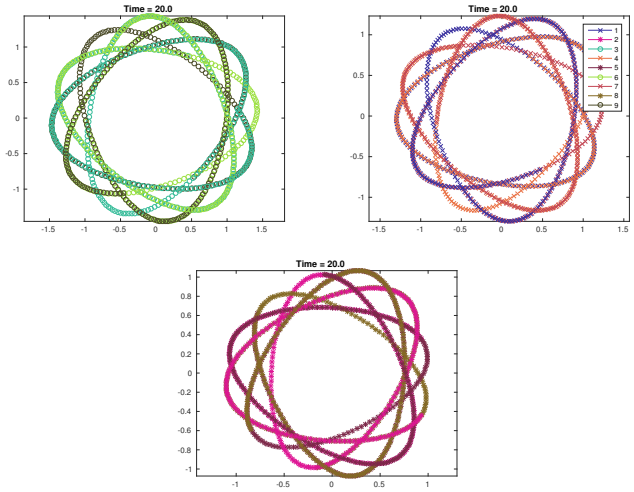

FIGURE 19. Isolated orbits of the evolution shown in Figure 18. Left: trajectories of agents 3, 6, 9. Middle: trajectories of agents 1, 4, 7. Right: trajectories of agents 2, 5, 8).

$x_{ij}(t) + C_2^j \tau$. This can be rewritten as:

$$\text{for all } i \in \{1, \dots, 4\}, \text{ for all } t > 0, \quad x_i(t+\tau) = x_i(t) + \begin{pmatrix} C_2^1 \\ C_2^2 \end{pmatrix} \tau.$$

□

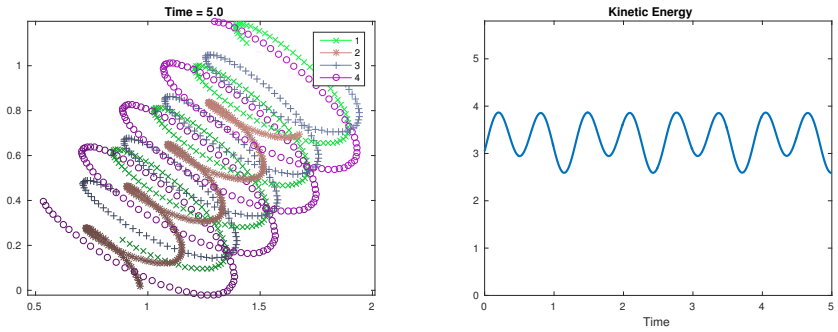

FIGURE 20. Left: Trajectories of 4 agents with helical trajectories. Parameters for matrix A (48) chosen to be $(a, b, c, d) = (1, 2, 3, 4)$. Dark to light color indicates earlier to later time. Right: Corresponding kinetic energy. The period is $\tau = 2\pi((a+c)(b+d))^{-1/2} = \pi/\sqrt{6}$ (see proof of Theorem 6.7).

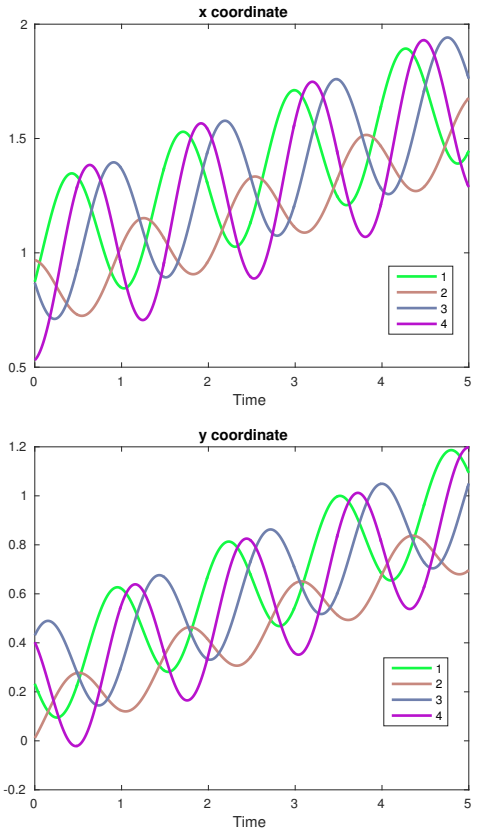

FIGURE 21. Evolution of the first and second coordinates of 4 agents with helical trajectories.

Theorem 6.8. *A system with helical trajectories has periodic kinetic energy.*

Proof. Supose that $(x_i)_{i=1\dots N}$ has helical trajectories, i.e. there exists $\tau \in \mathbb{R}$, $v \in \mathbb{R}^2$ such that for all $i \in \{1, \dots, N\}$, for all $t \geq 0$, $x_i(t+\tau) = x_i(t) + \tau v$. Then $\dot{x}_i(t+\tau) = \dot{x}_i(t)$ and so $E(t+\tau) = E(t)$. □

7. **Appendix.** An example using Approach A which shows unexpected behavior in the first example (A.1), as well as the interactions matrix and initial positions used for simulations shown in Figure 7 and 9.

Example 7.1. 15 agents with a general interaction matrix A. We use the same notion of a general interactions matrix as used in [3]. The interactions matrix A is composed of integers a_{ij} that are uniformly chosen between -5 and 5 inclusive. $\Psi \equiv \mathrm{Id}$. Generally, a system with this kind of interaction matrix will exhibit simple oscillating kinetic energy, as in [3]. We show a rare simulation using this general interactions matrix A in the appendix (Figures 22 and 23).

$$A = \begin{pmatrix} -5 & -1 & 1 & 0 & 4 \\ -1 & -5 & 1 & 1 & 0 \\ -2 & 0 & -5 & -1 & -2 \\ -4 & -1 & -5 & 3 & -4 \\ -4 & 1 & -2 & 2 & 1 \end{pmatrix} \qquad X = \begin{pmatrix} 1.5755 & 1.7399 \\ 1.6523 & 0.5619 \\ 5.3026 & 2.7008 \\ 2.4971 & 0.7288 \\ 0.6571 & 0.5281 \\ 1.2180 & 0.0840 \\ 2.2812 & 1.0129 \\ 5.4949 & 1.7441 \\ 3.7685 & 2.5903 \\ 1.6218 & 2.5266 \\ 2.2521 & 0.0767 \\ 5.5766 & 1.1671 \\ 5.6582 & 1.5453 \\ 2.8146 & 1.4641 \\ 1.6892 & 0.1310 \end{pmatrix}$$

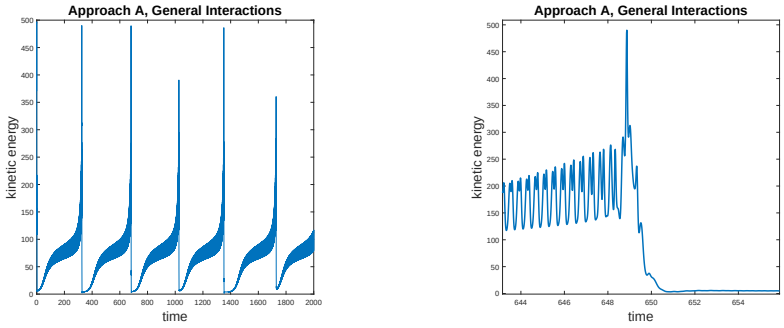

FIGURE 22. Energy of the system using Approach A, 15 agents, and a general interaction matrix (left). A snapshot of the energy oscillations to match with trajectories in Figure 23 (right).

Example 7.2. Five agents with a general interaction matrix A and Ψ as defined in (26). Simulations are shown in Figure 7 and 9 with $a \in \{\frac{\pi}{4}, \frac{\pi}{2}, \frac{3\pi}{4}\}$.

$$A = \begin{pmatrix} -5 & -1 & 1 & 0 & 4 \\ -1 & -5 & 1 & 1 & 0 \\ -2 & 0 & -5 & -1 & -2 \\ -4 & -1 & -5 & 3 & -4 \\ -4 & 1 & -2 & 2 & 1 \end{pmatrix} \qquad X = \begin{pmatrix} 6.1743 & 2.8473 \\ 4.5883 & 2.7635 \\ 2.1606 & 2.5691 \\ 3.6698 & 0.8191 \\ 0.6771 & 138672 \end{pmatrix}$$

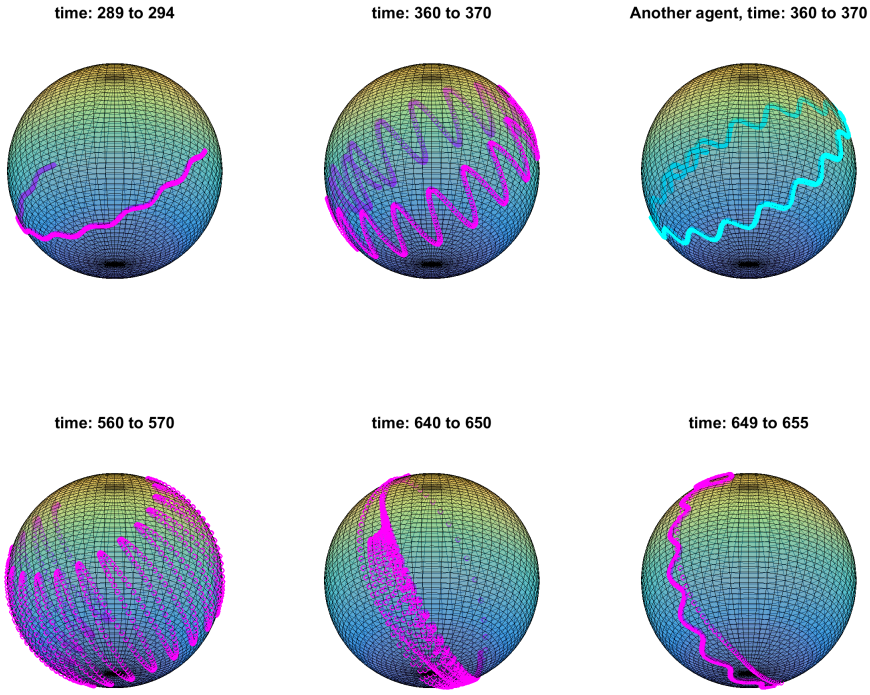

FIGURE 23. An agent's trajectory simulated with Approach A, 15 agents, and a general interaction matrix. The trajectory in shown the top right is of a second agent. The agents oscillate with amplitudes that increase with time, eventually the trajectory approximates a great circle, after which the oscillations resume with smaller amplitudes.

REFERENCES

[1] A. Aydoğdu, M. Caponigro, S. McQuade, B. Piccoli, N. Pouradier Duteil, F. Rossi and E. Trélat, Interaction network, state space and control in social dynamics, in *Active Particles Volume 1, Theory, Methods, and Applications* (eds. N. Bellomo, P. Degond and E. Tadmor), Birkhäuser-Springer, 2017.

[2] G. Bliss, The geodesic lines on the anchor ring, *Annals of Mathematics*, **4** (1902), 1–21.

[3] M. Caponigro, A. C. Lai and B. Piccoli, A nonlinear model of opinion formation on the sphere, *Discrete and Continuous Dynamical Systems - Series A*, **35** (2014), 4241–4268.

[4] J. Cheeger and D. G. Ebin, *Comparison Theorems in Riemannian Geometry, Vol. 365*, AMS Chelsea Publishing, 1975.

[5] D. Chi, S.-H. Choi and S.-Y. Ha, Emergent behaviors of a holonomic particle system on a sphere, *Journal of Mathematical Physics*, **55** (2014), 052703, 18pp.

[6] E. Cristiani, P. Frasca and B. Piccoli, Effects of anisotropic interactions on the structure of animal groups, *Journal of Mathematical Biology*, **62** (2011), 569–588.

[7] F. Dörfler, M. Chertkov and F. Bullo, Synchronization in complex oscillator networks and smart grids, *Proceedings of the National Academy of Sciences*, **110** (2013), 2005–2010.

[8] J. Gravesen, S. Markvorsen, R. Sinclair and M. Tanaka, *The Cut Locus of a Torus of Revolution*, Technical University of Denmark, Department of Mathematics, 2003.

[9] S.-Y. Ha, T. Ha and J. H. Kim, Emergent behavior of a Cucker-Smale type particle model with nonlinear velocity couplings, *IEEE Transactions on Automatic Control*, **55** (2010), 1679–1683.
[10] S.-Y. Ha, D. Ko, J. Park and X. Zhang, Collective synchronization of classical and quantum oscillators, *EMS Surveys in Mathematical Sciences*, **3** (2016), 209–267.
[11] R. Hegselmann and U. Krause, Opinion dynamics and bounded confidence: Models, analysis and simulation, *Journal of Artificial Societies and Social Simulation*, **5** (2002).
[12] Y. Kuramoto, Cooperative dynamics of oscillator community a study based on lattice of rings, *Progress of Theoretical Physics Supplement*, **79** (1984), 223–240.
[13] C. Moore, Braids in classical dynamics, *Physical Review Letters*, **70** (1993), 3675–3679.
[14] C. Moore and M. Nauenberg, New periodic orbits for the n-body problem, *ASME. J. Comput. Nonlinear Dynam.*, **1** (2006), 307–311.
[15] S. Motsch and E. Tadmor, Heterophilious dynamics enhances consensus, *SIAM Review*, **56** (2014), 577–621.
[16] A. Sarlette, S. Bonnabel and R. Sepulchre, Coordinated motion design on lie groups, *Automatic Control, IEEE Transactions on*, **55** (2010), 1047–1058.
[17] A. Sarlette and R. Sepulchre, Consensus optimization on manifolds, *SIAM Journal on Control and Optimization*, **48** (2009), 56–76.
[18] L. Scardovi, A. Sarlette and R. Sepulchre, Synchronization and balancing on the N-torus, *Sys. Cont. Let.*, **56** (2007), 335–341.
[19] R. Sepulchre, D. Paley and N. E. Leonard, et al, Stabilization of planar collective motion: All-to-all communication, *Automatic Control, IEEE Transactions on*, **52** (2007), 811–824.
[20] R. Sepulchre, D. Paley and N. E. Leonard, et al., Stabilization of planar collective motion with limited communication, *Automatic Control, IEEE Transactions on*, **53** (2008), 706–719.
[21] P. Sobkowicz, Modelling opinion formation with physics tools: Call for closer link with reality, *Journal of Artificial Societies and Social Simulation*, **12** (2009), p11.
[22] S. H. Strogatz, From Kuramoto to Crawford: Exploring the onset of synchronization in populations of coupled oscillators, *Physica D: Nonlinear Phenomena*, **143** (2000), 1–20.

Received March 2017; revised July 2017.

E-mail address: aylinvet87@gmail.com
E-mail address: sean.mcquade@rutgers.edu
E-mail address: nastassia.pouradierduteil@rutgers.edu